Mitigating high-temperature bleaching impacts on high-value corals using low-cost shading approaches, and assessments of a potentially novel coral disease affecting key reef building corals (phase 2)

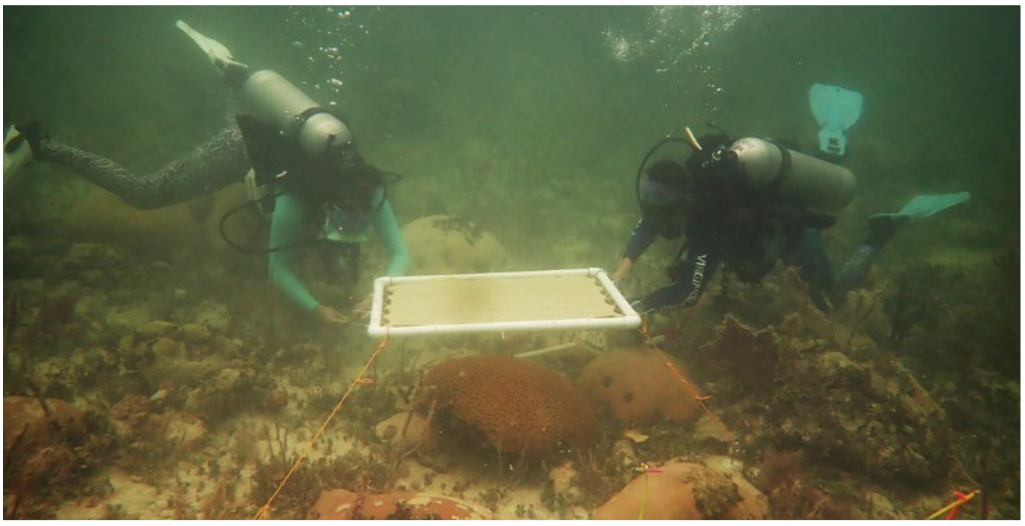

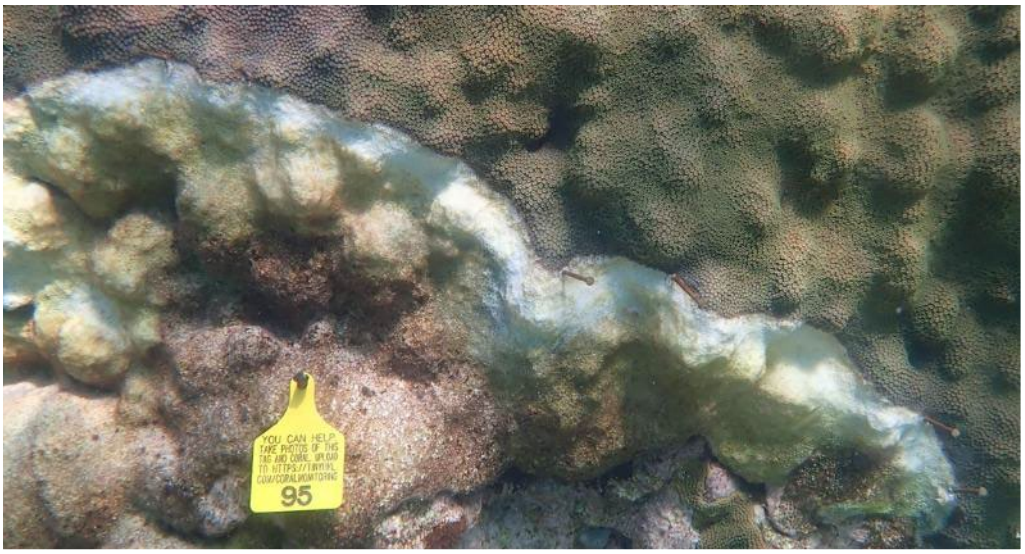

Mitigating high-temperature bleaching impacts on high-value corals using low-cost shading approaches, and assessments of a potentially novel coral disease affecting key reef building corals (phase 2)

Final Report

Prepared By:

Karen L. Neely[1], Arelys A. Chaparro[1], Kathryn A. Toth[1], Yasu Kiryu[2]

[1]National Coral Reef Institute, Nova Southeastern University, Dania Beach FL
[2]Fish and Wildlife Research Institute, Florida Fish and Wildlife Conservation Commission, St Petersburg FL

May 31, 2025

Completed in Fulfillment of PO C40144 for:

Florida Department of Environmental Protection
Coral Protection and Restoration Program
8000 N Ocean Dr.
Dania Beach, FL 33004

This report should be cited as follows:
Neely, KL. 2025. Mitigating high-temperature bleaching impacts on high-value corals using low-cost shading approaches, and assessments of a potentially novel coral disease affecting key reef building corals (phase 2). Florida DEP CPRP. Miami FL. 37 pp.

This report was funded through a contract agreement from the Florida Department of Environmental Protection's (DEP) Coral Protection and Restoration Program. The views, statements, findings, conclusions, and recommendations expressed herein are those of the author(s) and do not necessarily reflect the views of the State of Florida or any of its subagencies.

Acknowledgements

We are grateful to the members and labs of the *Orbicella* acute tissue loss disease working group for their collaborative efforts on assessing a potentially novel disease. We also thank Florida DEP for funding these projects. Bleaching shades were deployed and assessed under permits: FKNMS-2024-122, USACE SAJ-2024-01338, and FL DEP 44-0449369-001-EE. Assessments of OATLD lesions occurred under permit FKNMS-2023-141.

Management Summary (300 words or less)

Coral bleaching is an increasingly common stressor for reefs and can have substantial impacts on survival and future reproductive success. We found that temporary deployment of in-water shade structures on two brain coral species significantly minimized paling through the 2024 thermal stress event compared to unshaded controls. The shades performed well, exhibiting little fouling and remaining intact over several months. This method could be utilized to mitigate bleaching on priority corals during future warm water events.

Rapidly-progressing linear lesions affecting large *Orbicella faveolata* colonies in the Florida Keys led to the development of a consortium to assess these. As a result of synthesis of ongoing field and laboratory work, we suggest this is a potentially novel disease, present in the Florida Keys since at least 2019, which we term *Orbicella* acute tissue loss disease (OATLD). OATLD is characterized by histology which does not match the case definition for SCTLD, shows seasonal peaks and annual variability, and has rapidly progressing but regularly halting lesions. As this disease continues to destroy some of the largest and oldest animals in Florida, we strongly recommend further research, primarily to assess whether it is transmissible, whether other species can be affected, and whether treatment options can be developed.

Executive Summary (max 1 page)

Florida's Coral Reef continues to experience declines in live coral cover through a myriad of stressors, but two of the most impactful are hyperthermal events and coral disease. Neely lab projects from this funding cycle addressed these threats through testing in-water shading structures over bleaching-susceptible corals, and through a collaborative synthesis of field observations, histology, TEM, and microbiome work on a potentially novel disease affecting some of the largest corals in Florida.

The deployment of in-water shade structures over two species of brain coral (*Colpophyllia natans* and *Pseudodiploria clivosa*) at a nearshore Lower Keys site showed that shading did significantly minimize paling of these two species during the 2024 summer. Samples taken during regular monitoring are being analyzed for symbiont community structure by the Baker lab (University of Miami) and are expected to provide further insight. The impacts of bleaching to corals are not only immediate, but also have long-term effects like increased susceptibility to some diseases and reduced reproductive effort in subsequent years. Thus deployment of shades is also expected to have positive longer-term effects on protected corals. Shades were low-cost and held up well during their temporary three-month deployment. As such, they may be a useful tool for protecting targeted corals during future bleaching events.

Many of the largest *Orbicella faveolata* colonies in the Florida Keys have suffered extensive or total mortality from rapidly progessing linear lesions. During FY 2024-25, we collaboratively assessed field observations, histological studies, TEM observations, and microbiome analyses in order to better understand and describe these lesions, and as a result propose the name "*Orbicella* acute tissue loss disease" (OATLD). OATLD lesions had a different appearance than those of SCTLD, sometimes halted on their own, and were largely unaffected by amoxicillin application. Through historic assessment of intervention photos and data, these lesions were found to have been present since at least 2019 (before interventions were initiated), to peak in prevalence during late summer/early fall, and, concerningly, to disproportionately affect large corals. Histological examination shows that most of the characteristic traits of SCTLD (lytic necrosis and endosymbiont deformities) are not present in OATLD samples. Rather, OATLD samples are characterized by absent or necrotic mesenterial filaments, ghost symbionts, and degraded granular amoebocytes. TEM analyses are reported on in the Ushijima (UNCW) final report, but also found distinct differences from SCTLD, including high numbers of starch and lipids, as well as high numbers of accumulation bodies within the endosymbionts. Microbiome analyses are reported on in the Meyer (UF) final report, but in brief, found many ASVs that were similar between OATLD and SCTLD, but five bacterial taxa that are unique to OATLD. Overall, we conclude that OATLD is unlikely to be a variant of SCTLD, but instead a distinct disease that requires alternate management considerations. The consortium recommends prioritizing experimental testing of inter- and intraspecific transmissibility, and also trialing potential treatment options to prevent further loss of these large colonies.

Table of Contents

Required headings include:

- Background/Introduction: Brief summary of the project and why it is needed. Include a description of what work will be performed and/or completed with the DEP Funding.
- Methods: Must include detailed qualitative standards (who, how, when, where), and quantitative standards (minimum and maximum services provided).
- Results:
- Discussion and Management Recommendations: What is the management relationship to the results? What benefits have been provided by the Project?

1. TASK 1: MITIGATING BLEACHING IMPACTS USING SHADING

1.1. Background/Introduction

Coral loss from hyperthermal bleaching is recognized as one of the greatest threats to coral reefs worldwide, and is expected to become increasingly common and severe as climate change accelerates (Mellin et al. 2024). The 2023 summer marine heatwave in the Florida Keys once again highlighted the susceptibility of certain sites and species to bleaching related mortality (Neely et al. 2024). One potential action that can be taken to protect high-value corals is shading. Though shading does not impact cumulative heat stress, it does reduce UV and irradiance stress which has been shown to work in concert with and exacerbate bleaching impacts on coral colonies. Shading of colonies during bleaching events has been experimentally trialed in other coral reef regions (Tagliafico et al. 2022). Experiments outside of the Caribbean have found that shaded corals have delayed bleaching (Butcherine et al. 2023), have higher chlorophyll, symbiont density, and photosystem II protein (Jeans et al. 2013), and have higher growth rates (Coelho et al. 2017) than unshaded controls. During the 2023 Caribbean bleaching event, shade structures were deployed over 20 corals in Dominica (S. Walsh, pers comm), a few colonies in the Dry Tortugas (I. Kuffner, pers. comm.) and over some Florida Keys coral nursery shelves (Coral Restoration Foundation, Reef Renewal, pers. comm.).

Newfound Harbor, a patch reef off the Lower Keys, is prone to hyperthermal bleaching almost every year, largely due to the temperature extremes resulting from the shallow, inshore, bay-influenced nature of the reef (Manzello 2015). During the summer of 2023, losses to brain and boulder corals at the site were more severe than at all other regularly monitored sites within the Florida Keys National Marine Sanctuary. Partial and total mortality of brain corals was particularly pronounced, with between 41% - 80% of colonies of four brain coral species exhibiting losses (Neely et al. 2024). As such, we selected this site and these highly susceptible individuals to assess the use of shading structures on mitigating any 2024 bleaching at the site (Figure 1).

Our project goals asked two questions:

- Do corals shaded by artificial structures through a warm water event differ in bleaching severity and/or survival than non-shaded controls?
- Do corals shaded by artificial structures through a warm water event differ in symbiont:host ratios and symbiont community structure compared to non-shaded controls?

1.2. Methods

We selected two bleaching-susceptible species – *Colpophyllia natans* and *Pseudodiploria clivosa* - at Newfound Harbor, a site known to regularly experience high thermal stress. Selected colonies were of suitable size and shape for experimental shading, with each having at least one isolate exceeding 144 cm^2, but not bigger than 10,000 cm^2.

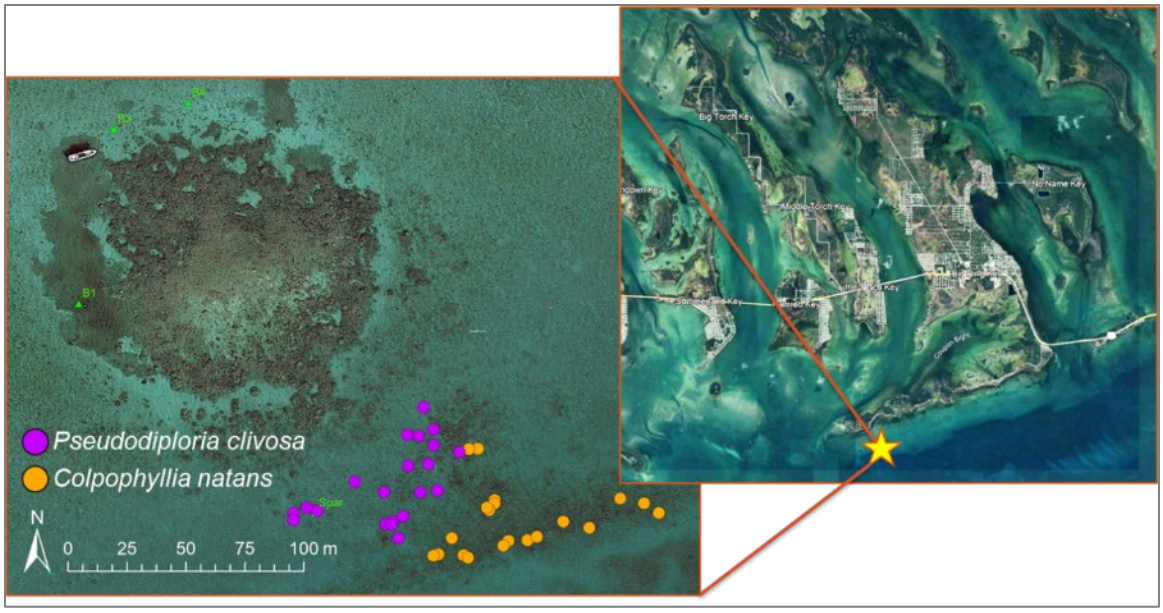

Figure 1: *The location of Newfound Harbor relative to Big Pine Key, Lower Florida Keys, and the location of the colonies of the two species (*Colpophyllia natans *and* Pseudodiploria clivosa*) within that area.*

Twenty colonies of each species were selected and divided into control (non-shaded) and experimental (shaded) treatments. Per permitting requirements, shaded corals could not be in proximity to each other, and so the experimental treatment corals were intentionally selected to be geographically dispersed across the site area, but otherwise corals were haphazardly sorted into treatment groups.

Shade structures consisted of polyvinyl chloride (PVC) frames, which were filled with spray foam for flotation and then sealed against water intrusion. Frames were sized for each individual coral. Agricultural shade cloth (60%) was attached internal to each frame using zip ties. Parachute cord was strung from the corners of each frame to eye screws which were affixed for the duration of the experiment into the substrate surrounding each shaded coral. Shades floated approximately 30 cm over the top of each target coral (Figure 2).

The experimental design called for deployment of the shades once cumulative thermal stress at the site reached 4 degree heating weeks (DHW), the expected onset of any paling/bleaching (Kayanne 2017). Unfortunately, permitting delays meant that shades could not be installed until DHWs were over 7. Additionally, we had to temporarily remove shade structures for two tropical storms (September 23 – October 1, and October 7 – October 14). Shades and all fixtures were removed when DHWs subsided to 4 on November 12.

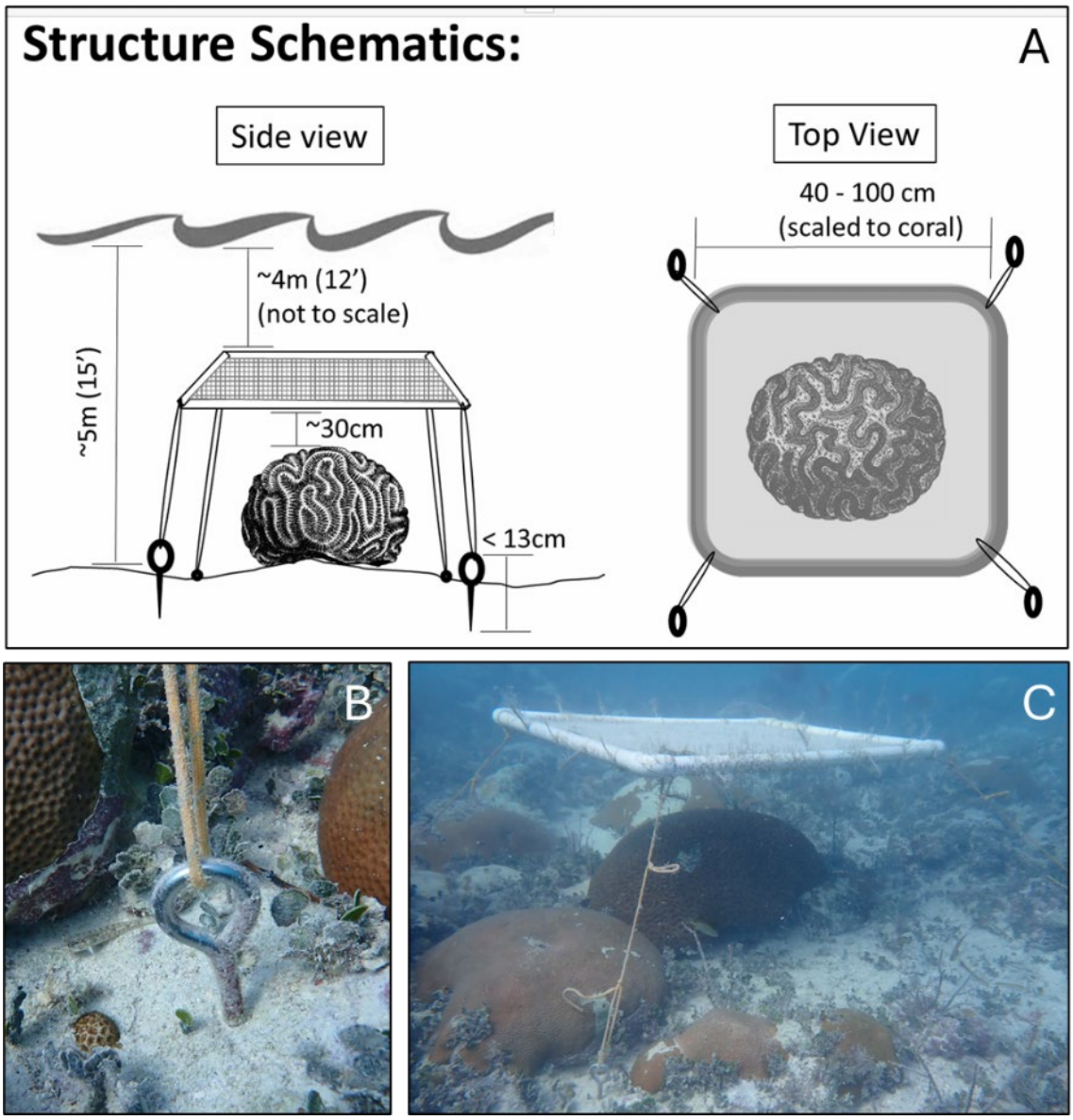

Figure 2: *Schematics of shade structures. Structures were rectangular foam-filled PVC frames with attached 60% agricultural shadecloth (A). Corners were attached with parachute cord to eyescrews screwed into the adjacent substrate (B). The structures were positively buoyant and tethered approximately 30 cm above the target corals (C).*

At least every two weeks, as well as when shades were removed or reinstalled for tropical storms, shades were lightly scrubbed to prevent fouling and additional shading. All shaded and control colonies were monitored and sampled. Corals were visually assessed for percent live cover and percent mortality. They were also assessed for paling/bleaching using a Coral Watch Coral Health Card (Figure 3). For each coral, the percentage of live coral that was paled/bleached was estimated, and the color index associated with that pale/bleach area was recorded. Additionally, the percentage of the coral that was not pale/bleached and its associated color index were recorded. These two values were averaged to provide a single bleaching index number for each colony using the equation:

$$\frac{(\%\ pale * pale\ index) + (\%\ nonpale * nonpale\ index)}{100}$$

Divers were permitted to record half-steps (eg. if the color was between a 3 and a 4, it could be recorded as 3.5).

Figure 3: *A Coral Watch Coral Health Card was used to assess the coloration of each colony. The card was held adjacent to normal and pale/bleached tissues and matched to the nearest color (with allowance for half steps).*

We analyzed the effects of treatment and time on bleaching index numbers using a Repeated Measures 2-way ANOVA. Data were first assessed for normality (Shapiro-Wilk) and equal variance (Brown-Forsythe). Post-hoc pairwise comparisons were conducted using Holm-Sidak tests. Each species was assessed independently.

During each monitoring period, we also used cuticle clippers to take a small tissue biopsy (approximately 2 mm^2) from the edge of each colony. The location of samples on each colony was standardized by taking samples adjacent to a nail placed adjacent to the initial sampling point. Each sample was put into a labelled bag and transferred into DNA/RNA Shield labeled tubes once topside. These fixed samples were transported to the Baker lab at University of Miami for symbiont analyses under their scope of work.

1.3. Results

1.3.1. Pseudodiploria clivosa

Among *Pseudodiploria clivosa* colonies, none experienced any partial or full mortality from bleaching nor any other stressor throughout the monitoring period.

For the coral bleaching index scores, treatment ($p = 0.01$), time ($p < 0.001$) and treatment x time ($p = 0.02$) were significant. Control corals were paler than shaded ones, with the three monitoring time points from September 13 – October 1 flagging as significant (Figure 4). This corresponds with the monitoring points during and immediately following bleaching alert level 2.

Corals had already begun paling by the time shades were deployed. Bleaching index scores during the first sampling points in mid-July averaged 3.7, while scores after waters had cooled (November 2024) were 4.9. Bleaching index scores further declined between the July monitoring period and the mid-August shade deployment date (control corals $p = 0.04$; shaded corals = 0.008). We thus cannot determine whether shading would have prevented any paling on this species. However, once shades were deployed, shaded colonies did not pale further while control colonies did.

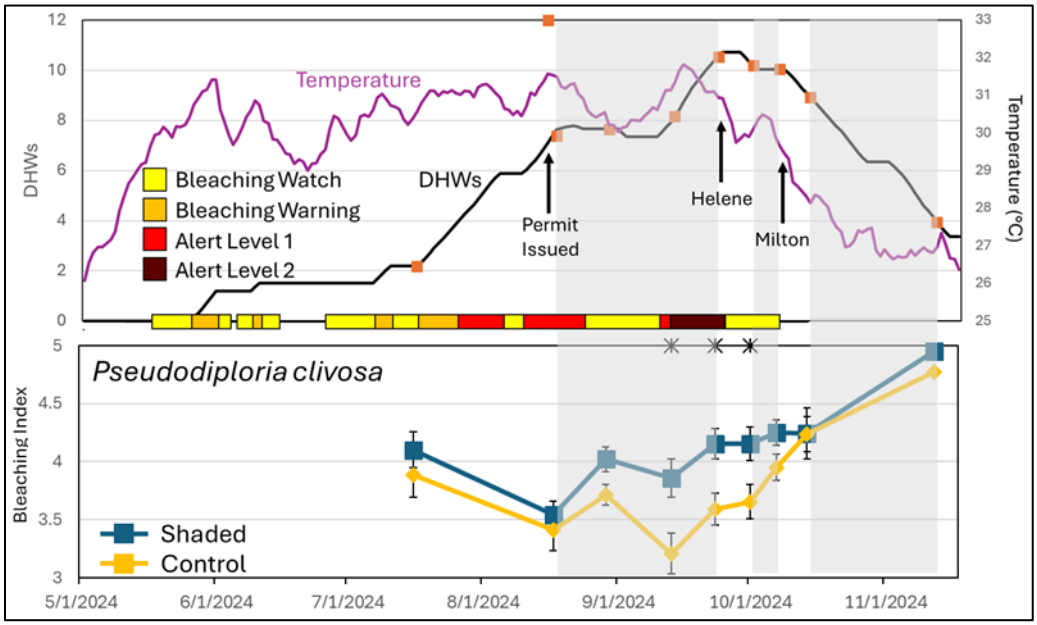

Figure 4: *The summer 2024 thermal regime at Newfound Harbor (top) and the bleaching index scores for* Pseudodiploria clivosa *colonies (bottom). Gray shaded bars indicate time points when the shades were deployed (including removal during two tropical storms), while orange squares (top) indicate monitoring time points. Temperature, degree heating weeks (DHWs) and bleaching alert level data are from the NOAA Coral Reef Watch single-pixel virtual station. Bleaching index scores (bottom) are shown for shaded (blue) and control (yellow) colonies, with error bars indicating standard error.*

1.3.2. Colpophyllia natans

Among *Colpophyllia natans* colonies, there was also no partial or total mortality from bleaching, nor from any other stressors, throughout the monitoring period.

For the coral bleaching index scores, treatment ($p = 0.003$) and time ($p < 0.001$) were both significant. The interaction of treatment x time was marginally significant ($p = 0.050$) and so interaction post-hoc tests were also run. Shaded corals were less bleached than control corals, with the four monitoring events between September 13 – October 7 flagging as significant. This corresponded to the two time points during the bleaching alert level two as well as the two subsequent monitoring events. The shaded *C. natans* corals did not have any significant changes in color through the hyperthermal event. Among the control corals, bleaching index values did change significantly through time.

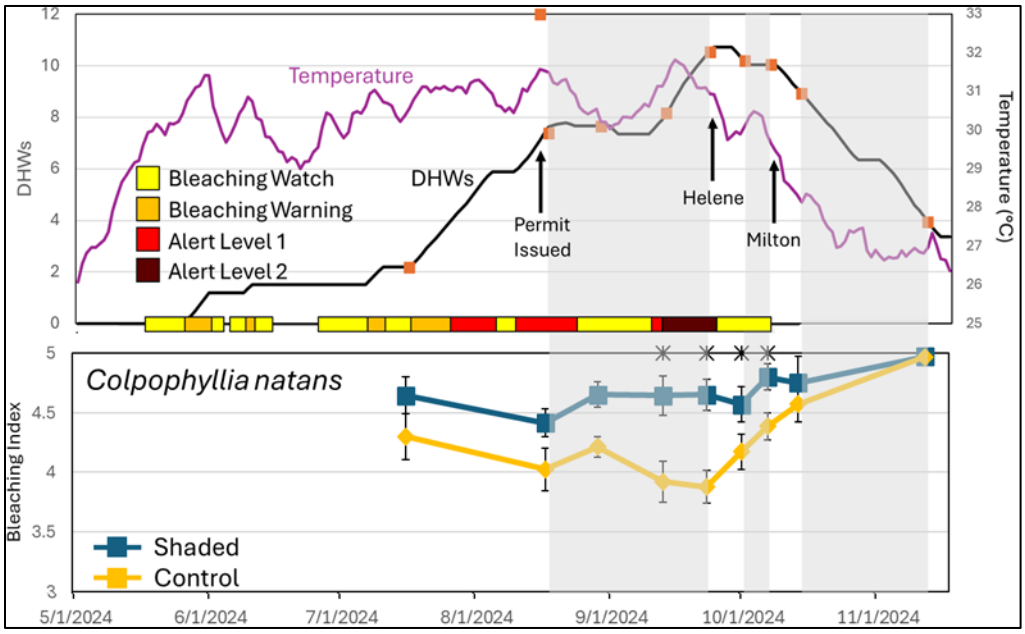

Figure 5: *The summer 2024 thermal regime at Newfound Harbor (top) and the bleaching index scores for* Colpophyllia natans *colonies (bottom). Gray shaded bars indicate time points when the shades were deployed (including removal during two tropical storms), while orange squares (top) indicate monitoring time points. Temperature, degree heating weeks (DHWs) and bleaching alert level data are from the NOAA Coral Reef Watch single-pixel virtual station. Bleaching index scores (bottom) are shown for shaded (blue) and control (yellow) colonies, with error bars indicating standard error.*

1.4. Discussion & Management Recommendations

The temporary installation of shade structures over corals at Newfound Harbor significantly reduced colony paling during the 2024 summer compared to controls. This treatment effect was driven by significant differences during the most thermally stressful time periods (8 – 10 DHWs). For *Colpophyllia natans*, bleaching index score remained unchanged from before the shades were deployed, while in control corals, colonies experienced significant paling. For *Pseudodiploria clivosa* colonies, even though shades were deployed after paling had already initiated, they were nevertheless impactful in preventing further paling, and also in promoting more rapid recovery compared to controls.

These metrics suggest that deployment of shades is an effective tool to minimize or prevent paling of Florida Keys corals, and that it can be effective even during minor bleaching/paling events. We also show that shading is beneficial even if deployed after paling has already initiated. Though no mortality was observed on control or experimental corals, minimizing or preventing paling is likely to still have positive health benefits for corals, including lower susceptibility to disease and higher reproductive capacity during the subsequent year (Levitan et al. 2014, Muller et al. 2018).

We found that the shade structures were surprisingly sturdy and remained largely unfouled through the experiment. Though structures were removed for two large wind events, there were other weather events through which they persisted with no damage. None of the eyescrews pulled out, and yet were easy to remove at the end of the experiment. Fouling of the shadecloth was minimal, with light sediment brushed off every two weeks but otherwise no major maintenance required.

We conclude that temporary deployment of shade structures could be successful in minimizing or preventing bleaching-related stress on targeted corals, even if deployed after paling has initiated. This may represent a low-cost effort to protect high priority corals from thermal stress and its subsequent effects.

2. TASK 2: ASSESSMENTS OF A POTENTIALLY NOVEL CORAL DISEASE AFFECTING KEY REEF BUILDING CORALS

2.1. Background/Introduction

Scleractinian corals are susceptible to a variety of stressors, but one of the most common and potentially devastating is disease. Though disease is present at background levels in all populations, outbreaks of disease can cause rapid and catastrophic losses of individuals as well as populations. The number and virulence of coral diseases has been steadily increasing (Porter et al. 2001, Burke et al. 2023), and disease is predicted to become even more common in the future (Maynard et al. 2015, Burke et al. 2023). The Caribbean basin is a hot spot for coral disease (Weil 2004), and major region-wide diseases such as white band disease (Gladfelter 1982) and stony coral tissue loss disease (Hawthorn et al. 2024) have resulted in widespread loss of corals, including near extinction of some species (Aronson and Precht 2001, Neely et al. 2021a).

Differentiating coral diseases presents challenges. Corals can only exhibit disease in so many ways, and the appearance of disease lesions can vary across individual colonies and species, and also through time (Aeby et al. 2021). Additionally, pathogen identification for most coral diseases has not been confirmed (Richardson 1998), meaning that even laboratory diagnostics cannot usually identify disease type. Nevertheless, identification of coral diseases remains important, especially in the field, for monitoring populations, tracking outbreaks and potentially applying disease treatments.

To better aid field identification, the Coral Disease and Health Consortium has proposed standardized nomenclature for lesion appearance and distribution across colonies (Rogers

2010). Additionally, laboratory tools to better identify diseases continue to be improved. These include microbiome analyses, histology, and TEM imaging (Gignoux-Wolfsohn et al. 2020, Landsberg et al. 2020, Papke et al. 2024).

We here assess and describe a potentially novel disease affecting corals in the Florida Keys. The disease is characterized by large, rapidly progressing lesions that appear only on *Orbicella faveolata* colonies, including some of the largest individuals on the reefs. Lesions are focal or multifocal and are typically linear, with distinct lesion edges and smooth margins (Figure 6). They are sometimes accompanied by an adjacent margin of dead tissue along the lesion edge. Lesions can progress in any direction across the colony, including horizontally, vertically, and diagonally. Following the terminology laid out by the Coral Disease and Health Consortium, we coin this syndrome **"Orbicella acute tissue loss disease" (OATLD).**

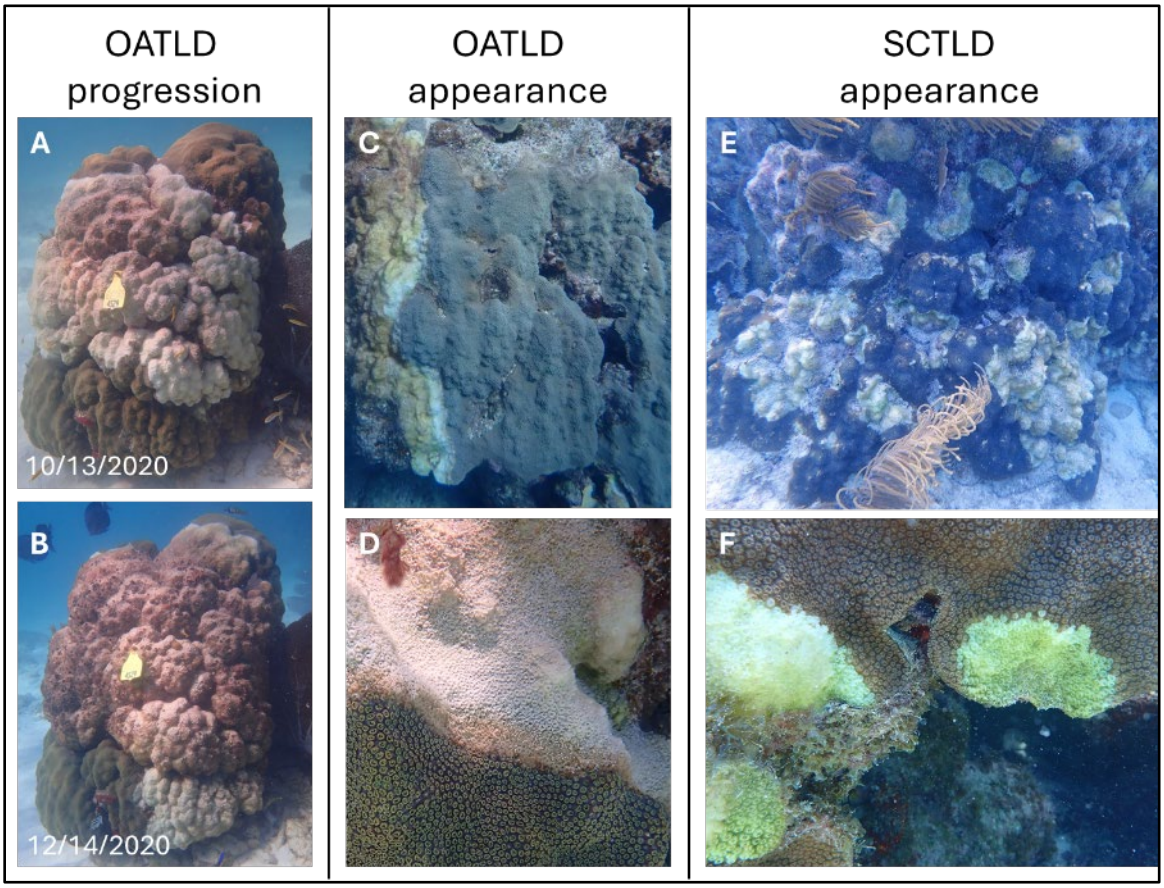

Figure 6: *Examples of* Orbicella faveolata *colonies exhibiting presumed OATLD lesions. Panels A and B show the progression of a lesion across a colony over 2 months. Panel C shows a lesion moving across a colony while panel D shows a close-up image of the lesion, including the occasionally-present band of degrading tissue. Panels E and F show zoomed out and zoomed in images of traditional SCTLD lesions for comparison.*

These lesions share some similarity to the description of white plague type III in Richardson et al. (2001). White plague type III was described as causing extremely rapid tissue loss on large corals, specifically *Colpophyllia* spp. and *Orbicella faveolata*

(lumped into the *annularis* species complex in Richardson) in the Caribbean. Descriptions for this white plague type III vary, with observations of lesions progressing from the center of colonies (Bythell et al., 2004), as well as from the base (Chaves-Fonnegra et al., 2021). However, the white plague type III nomenclature was discarded due to inconsistent pathogen identification, with only white plague type I and type II considered valid (Croquer et al., 2021). Early investigations of the corals assessed recently in Florida colloquially called these lesions "fast lesion progression (FLP)" (https://www.agrra.org/wp-content/uploads/2023/03/FLP-Report_Neely_20230321.pdf), but this term has been discarded as well for the new OATLD terminology.

During the 2023-24 fiscal year, the Nova Southeastern University (NSU) Florida Keys Strike Team received Florida Department of Environmental Protection (DEP) funding to identify and tag afflicted colonies at three Florida Keys sites, to measure lesion progression rates, to assess historical presence of this potentially novel disease using 2019 photographs, and to use photographs to look at historical treatment efficacy. Also, as part of this funding, samples of affected colonies and relevant controls were collected for histological (Kiryu – Florida Fish and Wildlife Conservation Commission (FWC)), Transmission Electron Microscopy (TEM) (Ushijima – University of North Carolina Wilmington (UNCW)), and microbiome (Meyer – University of Florida (UF)) analyses. As part of the 2024-25 fiscal year, UNCW and UF teams were funded to analyze these samples under their own scopes of work (and are shared as part of their final reports). FWC and NSU analyses were conducted pro bono. DEP funding also supported semi-monthly virtual meetings as well as an in-person workshop to synthesize the results of the teams' analyses.

2.2. Methods

2.2.1. Field Observations (NSU)

2.2.1.1 Lesion tracking

Though not part of this project's funding, we regularly monitored OATLD-affected corals at three sites within the Florida Keys National Marine Sanctuary: the paired Carysfort South and Carysfort Main reefs, the Grecian/Key Largo Dry Rocks (KLDR) paired reefs, and Looe Key (Figure 7). Corals with presumed OATLD were tagged and mapped, measured for straight line length, width, and height, assessed for percent live, recently dead, and old dead coverage, and photographed. On active lesions, two nails were placed on the live/dead tissue margin 10 cm apart from each other. For lesions longer than 50 cm, multiple nail sets were placed along the lesion line, each at least 20 cm apart from the neighboring set.

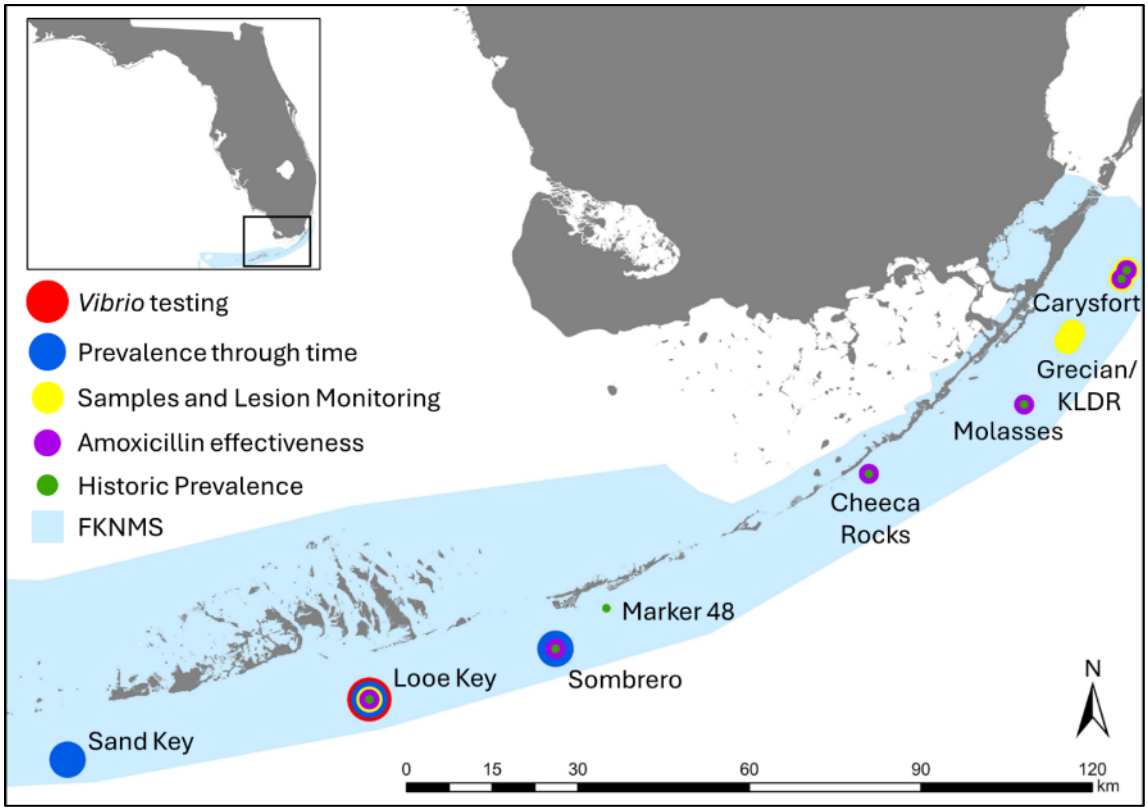

Figure 7: *Map of sites within the Florida Keys where OATLD work or historical imagery analysis occurred.*

Each site was visited approximately every two months from January 2024 to January 2025. During each visit, any newly affected corals with measurable lesions were tagged and measured as above. Any previously tagged corals were assessed for percent live, old dead, and recently dead. Any previous lesions were assessed as active, halted, or no longer present because all previously live tissue ahead of the lesion was dead. Lesion progression rates for active lesions were measured as the distance the lesion had progressed perpendicular to the marker nails divided by the number of days since the previous observation (cm / day).

We obtained a total of 122 OATLD lesion measurements from 60 affected corals across the three sites. This included 14 colonies at Carysfort, 17 at Grecian/KLDR, and 29 at Looe Key. Lesion progression rates between sites were compared using a One-Way ANOVA. Proportions of halted lesions between sites were compared using a Chi-squared test.

2.2.1.2 Amoxicillin effectiveness

A topical amoxicillin paste (98% amoxicillin trihydrate mixed with Ocean Alchemist Base2b in a 1:8 by weight ratio) is widely used to treat SCTLD lesions (Neely et al. 2021b, Toth et al. 2024). Using the historical imagery outlined above from corals that were determined to in fact have OATLD lesions rather than SCLTD ones, we assessed whether efficacy of the amoxicillin treatment was similar for OATLD lesions. From corals at five reef sites (Looe Key, Sombrero, Cheeca Rocks, Molasses, and Carysfort)

we assessed 40 OATLD lesions treated in 2019-2020 and 23 lesions treated in 2022-2023. Treatment efficacy was assessed by comparing the initial treatment photos with lesion photos from the subsequent monitoring (no more than three months after treatment). Effective treatment was defined as the lesion halting at the treatment line, while ineffective treatment was defined as the lesion continuing past the treatment line. The proportion of OATLD lesion treatments that responded to treatments were compared using generalized linear models assessing site, time period (2019-2020 vs 2022-2023), and the interaction between the two. We chose the best model based on Akaike Information Criterion scores and conducted emmeans post-hoc tests.

2.2.1.3. Historical presence

We used photographs from 2019 – 2023 to determine whether OATLD was present at Florida Keys reef sites in past years. Photographs were taken as a component of the intervention response to the SCTLD outbreak. As part of that response, over 5000 corals in the Florida Keys National Marine Sanctuary were treated for disease (Neely et al. 2021b). Treatments included a topical amoxicillin paste, chlorinated epoxy, topical antimicrobials, and/or probiotics. During the SCTLD outbreak, it was presumed that any white lesions were SCTLD and treated accordingly. For each treated coral, photos were taken before the initial treatments, and these were revisited to determine to what extent lesions now presumed to be OATLD were present during past years

2.2.1.4. Colony size

In order to assess whether colony size affected the probability of developing OATLD, the maximum dimension of *O. faveolata* colonies affected with OATLD at least once in their monitoring history was compared with the maximum dimension of other tagged *O. faveolata* colonies never recorded to be affected with OATLD at three offshore sites (Looe Key N =716, Sombrero N = 78, and Sand Key N = 130). Because maximum diameters were not normally distributed (Shapiro test), we used Wilcoxon-Rank tests to compare the two groups.

2.2.1.5. Seasonal assessments

At three offshore sites with large numbers of *O. faveolata* colonies (Sombrero, Looe Key, Sand Key), photographs of each *O. faveolata* colony from each monitoring period were assessed to identify whether any lesions were SCTLD, OATLD, or both. Because each site was fully surveyed during every monitoring period and all newly diseased corals were tagged and subsequently monitored, we made the assumption that the number of *O. faveolata* colonies at the conclusion of monitoring (July 2024) was the total number of known susceptible colonies to SCLTD and/or OATLD. For each monitoring period, we divided the number of colonies affected by OATLD by this total number of colonies. However, if a colony died or went permanently missing, we excluded it from the denominator (total number) for the month of death and all subsequent months. For each monitoring period, we also excluded any colonies that were specifically noted as not found during that monitoring event.

To determine if there was a seasonal pattern to the prevalence of OATLD on reefs, the months that colonies were affected with OATLD were first converted to angles. Rayleigh tests of uniformity were then performed on the data to determine if there was a significant seasonality component. Analyses were conducted using the *circular* package in R version 4.4.3.

2.2.1.6. *Vibrio* presence

At Looe Key, we tested five apparent OATLD lesions and five apparent SCTLD lesions for the presence of *Vibrio coralliilyticus*, a pathogen typically associated with coral diseases and known to exacerbate the progression rates of SCTLD (Ushijima et al. 2020). We used 10cc syringes to agitate the lesion margin and collect the mucus/tissue slurry, which were then dripped onto the testing kits developed in Ushijima et al. (2020).

2.2.2. Histology (FWC – provided by Yasu Kiryu)

2.2.2.1. Sample collection

A total of 39 *Orbicella faveolata* core samples, each 2.5-cm in diameter, were collected from three sites – Carysfort, Grecian/KLDR, and Looe Key, in late January 2025. At each site, five diseased colonies were selected, and two cores were biopsy punched per colony – one from affected (disease affected; DA) and one from unaffected (disease unaffected; DU), separated by approximately 30 – 50 cm. DA samples were collected from the leading-edge border of the apparent tissue loss progression. An additional core was taken from each of three healthy colonies (HH). All samples were fixed with 20% Z-Fix (Anatech Ltd. Battle Creek, MI) for histological analysis and transported to FWC-FWRI Lab at St. Petersburg, FL.

2.2.2.2 Histological processing

All fixed samples were archived and FWRI's accession numbers were given to each sample in addition to field IDs. Prior to processing samples for histological slides, the external surface area was examined under a dissecting microscope, particularly focusing on presence or absence of the mesenterial filaments protrusion from the surface tissue. Photomicrographs were taken for all samples at low and high magnifications. Then, all the samples were decalcified in 10% ethylenediaminetetraacetic acid (EDTA) solution, requiring an average of 28 days (SD ± 3.7 d; range 19 – 37 d; n = 39). Decalcified tissues were oriented for sectioning at both radial (cross, parallel to the polyp mouth) and sagittal (longitudinal, perpendicular to the polyp mouth) angles. Routine paraffin-embedded histologic sections were sectioned at 4 µm, stained with Mayer's hematoxylin and eosin (H&E), thionin, and Giemsa (Luna 1968). Tissues were also embedded with glycol methacrylate plastic resin (JB-4; Electron Microscopy Sciences, Hatfield, PA) with arbitrary angle, sectioned at 4 µm, and stained with Weigert's H&E, thionin, and periodic acid–Schiff–metanil yellow (PAS-MY; Quintero-Hunter et al. (1991)). Slides were examined using light microscopy. Histopathological parameters were recorded for presence or absence and described separately by host anatomical tissue locations and endosymbionts.

2.2.2.3 Statistical analysis

Fisher's exact tests with Bonferroni adjusted p-values were used to compare the prevalence of the gross pathological and histopathological variables, with pairwise comparisons conducted for disease conditions and sampling sites.

2.2.3. Collaborative Meetings

The collaborative team consisted of field observations (Neely lab – NSU), histology (Kiryu lab – FWC), TEM (Ushijima lab – UNCW), and microbiome (Meyer lab – UF). The group met via online platforms every other month (August 2024, October 2024, December 2024, February 2025, April 2025) and as an in-person workshop in May 2025.

2.3. Results

2.3.1. Field Observations (NSU)

2.3.1.1 Lesion tracking

Of the 122 lesion measurements taken across all three sites, 54 (44%) halted between visits. There was no significant difference in the proportion of lesions halted among sites ($\chi^{2\ (2,\ N\ =\ 122)} = 4.8$, $p = 0.09$). Of these halted lesions, 9.3% (5/54) had 0 centimeters of lesion growth between monitoring visits, indicating that lesions halted directly after the monitoring visit. (Figure 8A). The proportion of lesions that halted did not exhibit any seasonal pattern (Figure 8B).

Lesion progression rates averaged 0.43 cm/day, with a range of 0.1 - 1cm per day. Progression rates were not significantly different between sites (One-Way ANOVA; $F = 0.37$, $p = 0.69$. Figure 8C).

2.3.1.2 Amoxicillin effectiveness

Of the 66 amoxicillin-treated OATLD lesions assessed, 33% halted at the treatment line (Figure 8D). A series of generalized linear models were fitted to assess the effects of time (2019-2020 vs 2022-2023) and site, as well as their interaction, on the effectiveness of the amoxicillin treatment. The model that included the interaction effect identified no effect of site ($p = 0.5$), significantly higher efficacy of 2019-2020 treatments than the 2022-2023 treatments ($\chi^2 = 4.73$, $df = 1$, $p = 0.03$), and a significant interaction effect between site and time period ($p = 0.04$). The best GLM model included only time (AIC = 84.1).

2.3.1.3. Historical presence

OATLD was present on some of the first 40 *O. faveolata* (34 at Molasses) visited and treated at all six monitoring sites (Figure 8E). At four of the six sites, a few corals exhibited both OATLD and SCTLD-style lesions. The proportion of colonies with OATLD lesions ranged from 5% (Marker 48) to 42% (Molasses). The proportion of OATLD-affected colonies differed significantly among sites, ($\chi^{2\ (5,\ N\ =\ 234)} = 22.5$, $p < 0.001$).

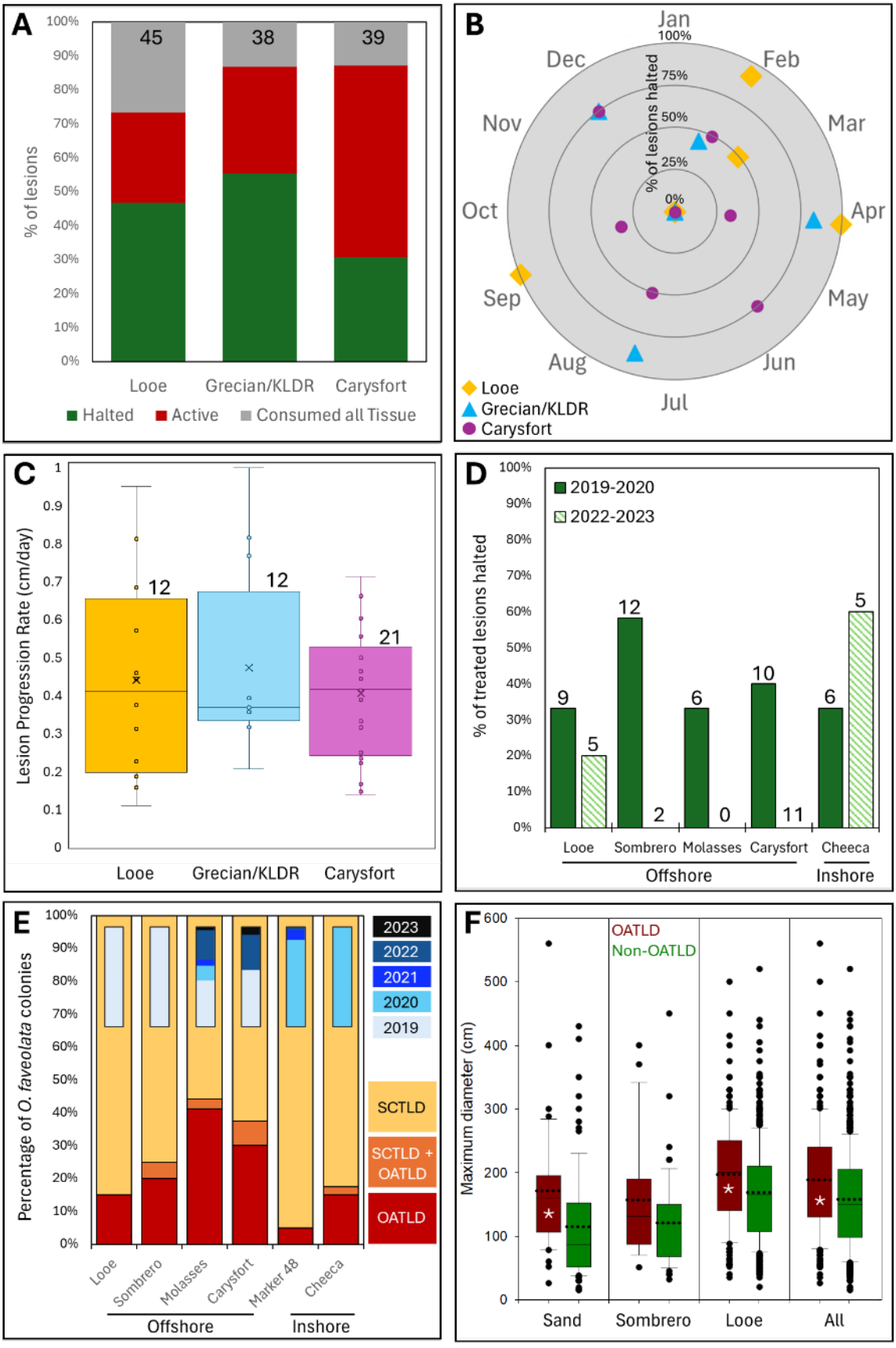
A
100%
90%
80%
70%
60%
50%
40%
30%
20%
10%
0%
% of lesions
45
38
39
Looe
Grecian/KLDR
Carysfort
Halted
Active
Consumed all Tissue
B
Jan
Feb
Mar
Apr
May
Jun
Jul
Aug
Sep
Oct
Nov
Dec
100%
75%
50%
25%
0%
% of lesions halted
Looe
Grecian/KLDR
Carysfort
C
Lesion Progression Rate (cm/day)
1
0.9
0.8
0.7
0.6
0.5
0.4
0.3
0.2
0.1
0
12
12
21
Looe
Grecian/KLDR
Carysfort
D
% of treated lesions halted
2019-2020
2022-2023
9
5
12
2
6
0
10
11
6
5
Looe
Sombrero
Molasses
Carysfort
Cheeca
Offshore
Inshore
E
Percentage of O. faveolata colonies
2023
2022
2021
2020
2019
SCTLD
SCTLD + OATLD
OATLD
Looe
Sombrero
Molasses
Carysfort
Marker 48
Cheeca
Offshore
Inshore
F
Maximum diameter (cm)
OATLD
Non-OATLD
Sand
Sombrero
Looe
All

Figure 8: *(A) The proportion of tracked OATLD lesions on* Orbicella faveolata *colonies that halted, remained active, or consumed all available tissue within two months. (B) The proportion of tracked lesions that halted during each monitoring time point, showing no seasonal component to halting. (C) The daily progression rate of active OATLD lesions. (D) The percentage of amoxicillin-treated OATLD lesions that halted at the treatment line, separated by site as well as treatment date (2019-2020 vs 2022-2023). For all figures, numbers indicate sample sizes. (E) The percentage of the first 40* O. faveolata *colonies (only 34 at Molasses) treated under Florida Keys strike team efforts that in fact had OATLD lesions, separated by site. (F) The maximum diameter of* O. faveolata *colonies affected by OATLD lesions at some point as compared to those only affected by SCTLD. The asterisks indicate significantly greater average size of OATLD-affected corals at two sites and overall as compared to SCLTD-affected colonies.*

2.3.1.4. Colony Size

O. faveolata colonies that were affected with OATLD at least once between 2019 and 2023 were significantly larger than colonies with only SCTLD (Figure 8F). Across all three sites, OATLD-affected colonies averaged 189 ± 87 cm in maximum diameter, while non-OATLD colonies averaged 158 ± 80 cm ($p < 0.001$).

2.3.1.5. Seasonal assessments

The number of tagged *O. faveolata* with OATLD was assessed during each monitoring period. There was a significant seasonality in the number of corals affected, peaking in October when summed across all sites (Rayleigh test of uniformity: $r = 0.27$, $p < 0.0001$). Peak prevalence varied slightly by site, with a non-significant peak in September at Sombrero ($p = 0.28$), a significant peak in October at Sand Key ($p < 0.005$), and a significant peak in November at Looe Key ($p < 0.0001$)(Figure 9). These seasonal outbreaks also varied by year, with most affected corals at Sand Key in 2021, Sombrero in 2020, and Looe Key in 2021 and 2022. Though seasonal peaks were focused during annual periods of highest cumulative thermal stress, the presence of OATLD essentially disappeared during the extreme bleaching event in the summer of 2023.

2.3.1.6 *Vibrio* presence

All five OATLD lesions tested negative for *V. coralliilyticus*, while four of the five SCTLD lesions tested negative for the pathogen. The remaining SCTLD lesion had an irregular result and we could not determine presence/absence. There is no indication that *V. coralliilyticus* is associated with OATLD lesions nor of any of the tested SCTLD lesions.

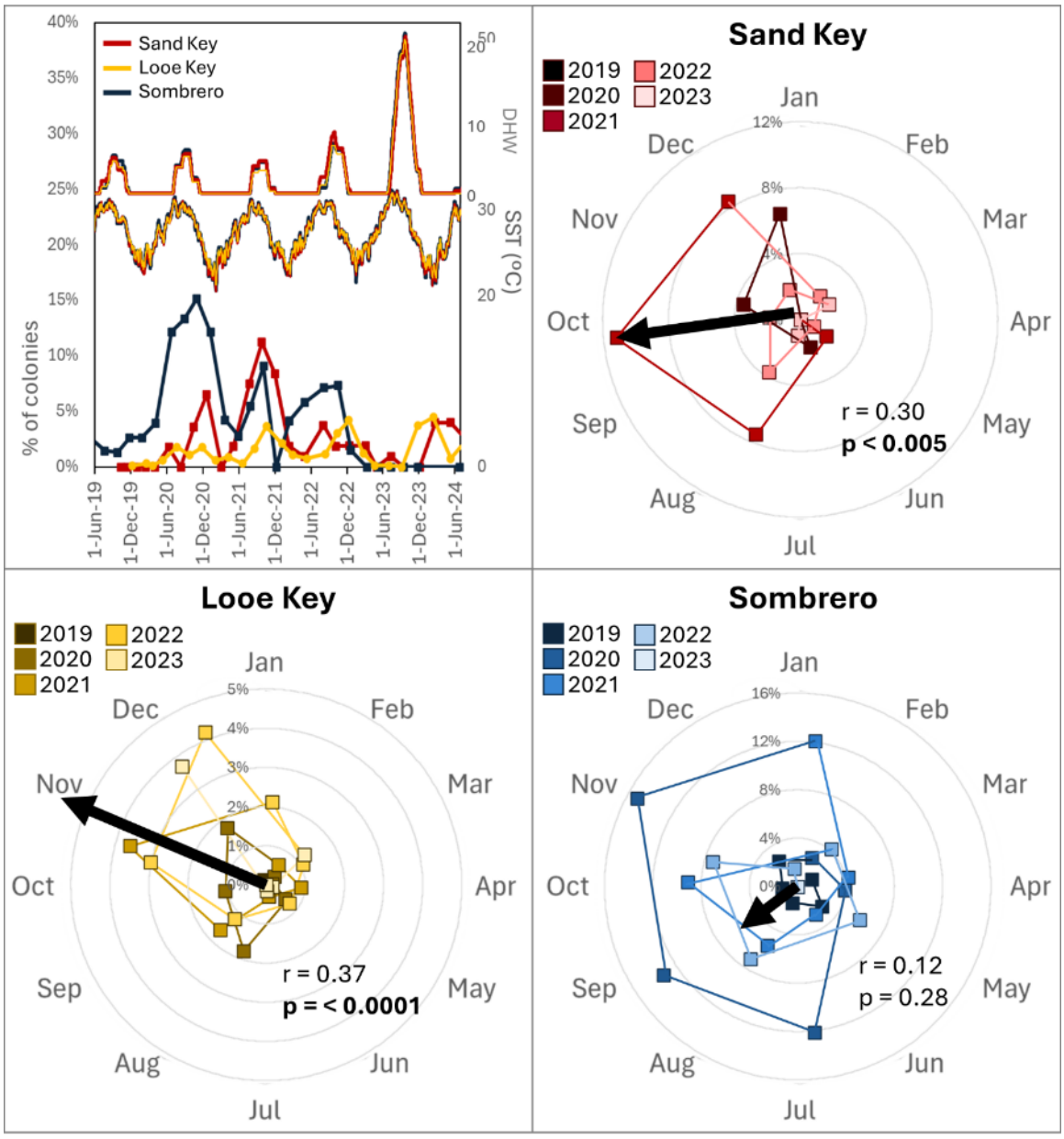

Figure 9: *The proportion of tagged* Orbicella faveolata *colonies with active OATLD lesions through time. Prevalence on a linear time scale shows seasonal and annual variation, with sea surface temperatures and degree heating weeks for each site also indicated (data from NOAA Coral Reef Watch). Prevalence on annual circular plots shows the magnitude of annual outbreaks, the near absence of OATLD lesions from January – June, and seasonal peaks in September – November. Arrows represent the vector of peak prevalence, with the length of the arrow indicating the strength of the vector (r), and the p-value indicating whether seasonality differed from random.*

2.3.2. Histology (FWC – provided by Yasu Kiryu)

2.3.2.1. Protruded mesenterial filaments

The macroscopic observance of protruded mesenterial filaments was significantly less frequent in DA (27%). However, there was no statistical difference between HH (100%) and DU (87%) (Figure 10). There was no statistically significant difference among sites (Table 1).

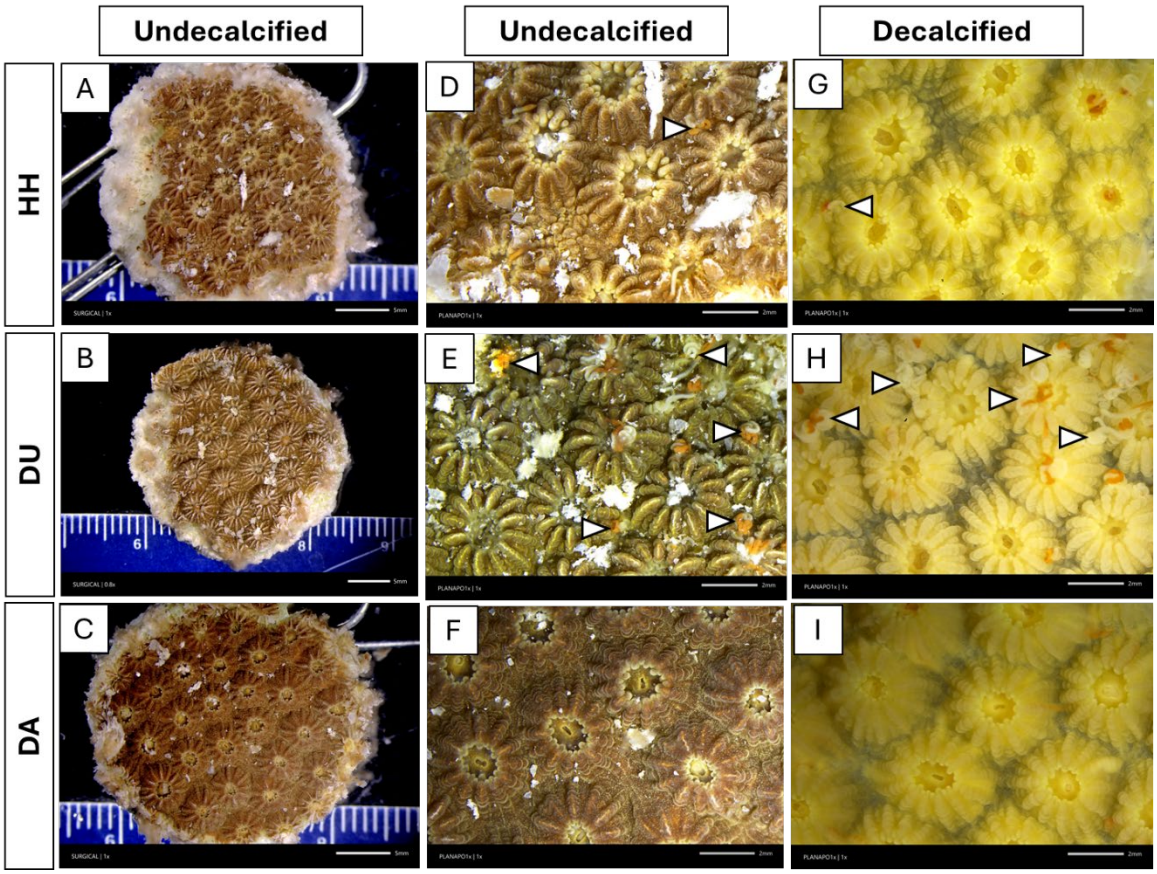

Figure 10. *Post-fixed macrophotographs of* Orbicella faveolata *core samples taken prior to histological slide processing. (A) A core sample from a healthy colony. (B) A core sample from a disease unaffected colony. (C) A core sample from a disease affected area of the same colony as (B). (D) High magnification of (A) showing a light amount of mesenterial filament protrusion (arrowhead). (E) High magnification of (B) showing a moderate amount of mesenterial filament protrusion (arrowheads). (F) High magnification of (C) showing no mesenterial filament protrusion. (G) Decalcification of (D) showing a light amount of mesenterial filament protrusion (arrowhead). (H) Decalcification of (E) showing moderate amount of mesenterial filament protrusion (arrowheads). (I) Decalcification of (F) showing no mesenterial filaments. All samples were obtained from Carysfort.*

Health Status	Carysfort	Grecian/KLDR	Looe	Total
HH	100% (3/3)	100% (3/3)	100% (3/3)	100% (9/9)[a]
DU	60% (3/5)	100% (5/5)	100% (5/5)	87% (13/15)[a]
DA	0% (0/5)	40% (2/5)	40% (2/5)	27% (4/15)[b]
Total	46% (6/13) [ns]	77% (10/13) [ns]	77% (10/13)[ns]	37% (26/39)

Table 1. *Prevalence of protruded mesenterial filaments observed under a dissecting scope in post-fixed Orbicella faveolata specimens collected in January 2024 from the three sites in Florida. Health conditions: HH, healthy; DU, disease unaffected; DA, disease affected. Fisher's Exact test adjusted p-value ($p < 0.05$) indicated by letters a, b, and not significant (ns).*

2.3.2.2. Degraded granular amoebocytes (globules)

Granular amoebocytes were degraded in the mesenterial filaments adjacent to the cnidoglandular band (Figure 11 A–B). The globules were commonly rounded, spherical, globular in shape, and approximately 10 µm diameter (ranging from 7.5 – 12.5 µm), with a homogeneously flat to bumpy appearance. They stained eosinophilic to brownish under H&E, and occasionally possessed demarcated, thickened eosinophilic stained outer rings. Globules were found in the mesenterial filaments throughout the coelenteric cavities of polyp, and they were also detected in the externally protruded mesenterial filaments. Degraded granular amoebocytes were significantly more frequent in DA (93%), while DU (33%) and HH (0%) were not significantly different (Table 2).

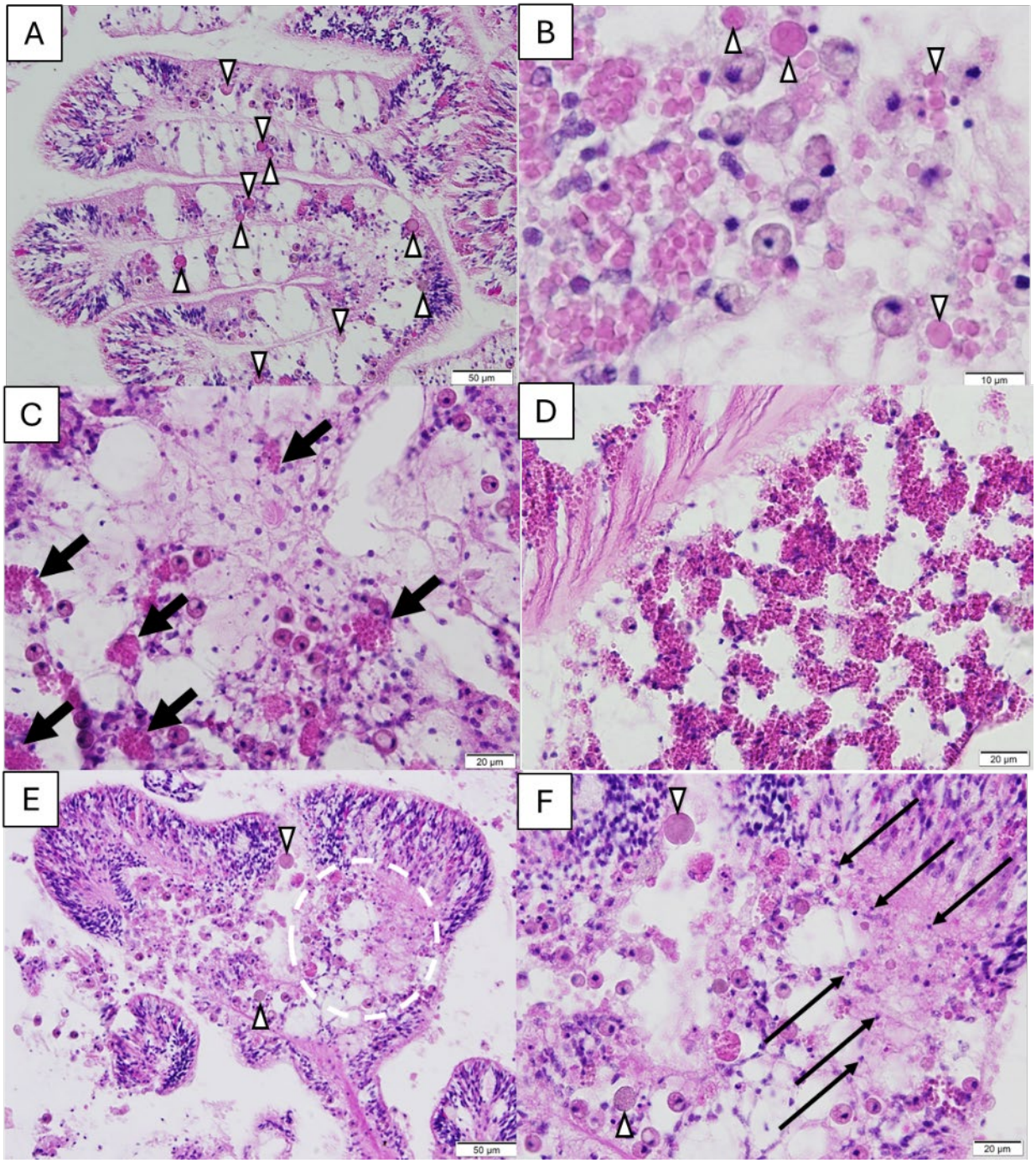

Figure 11. *Histological sections of* Orbicella faveolata *(H&E). (A) Degraded granular amoebocytes (globule; arrowheads) in the mesenterial filaments of a disease affected colony. (B) High magnification of degraded granular amoebocytes (arrowheads) in a disease affected colony. (C) Aggregation (depletion) of granular amoebocytes (arrows) in a disease affected colony. (D) Healthy, abundant granular amoebocytes in a specimen from heathy colony. (E) Necrosis (dotted circle) of mesenterial filaments associated with degraded granular amoebocytes (arrowheads) in a disease affected colony. (F) High magnification of dotted circle area in (E) showing karyorrhexis (arrows) and degraded granular amoebocytes (arrowheads). All samples were obtained from Carysfort.*

Health Status	Carysfort	Grecian/KLDR	Looe	Total
HH	0% (0/3)	0% (0/3)	0% (0/3)	0% (0/9) [a]
DU	40% (2/5)	20% (1/5)	40% (2/5)	33% (5/15)[a]
DA	100% (5/5)	80% (4/5)	100% (5/5)	93% (14/15)[b]
Total	54% (7/13) [ns]	38% (5/13) [ns]	54% (7/13)[ns]	49% (19/39)

Table 2. *Prevalence of degraded granular amoebocytes in the mesenterial filaments of* Orbicella faveolata*. Health conditions: HH, healthy; DU, disease unaffected; DA, disease affected. Fisher's Exact test adjusted p-value ($p < 0.05$) indicated by letters a, b, and not significant (ns).*

2.3.2.3. Aggregated (depleted) granular amoebocytes

Aggregated granular amoebocytes (Figure 11C) in the mesenterial filaments (mainly at the coelenteric cavities) were significantly more frequent in DA (100%) compared to DU (27%) and HH (22%), with no significant difference between DU and HH (Table 3) as healthy specimens contain abundant granular amoebocytes (Figure 11D).

Health Status	Carysfort	Grecian/KLDR	Looe	Total
HH	33% (1/3)	0% (0/3)	33% (1/3)	22% (2/9) [a]
DU	0% (0/5)	40% (2/5)	40% (2/5)	27% (4/15)[a]
DA	100% (5/5)	100% (5/5)	100% (5/5)	100% (15/15)[b]
Total	46% (6/13) [ns]	54% (7/13) [ns]	62% (8/13)[ns]	54% (21/39)

Table 3. *Granular amoebocyte aggregation (depletion) in the mesenterial filaments of* Orbicella faveolata*. Health conditions: HH, healthy; DU, disease unaffected; DA, disease affected. Fisher's Exact test adjusted p-value ($p < 0.05$) indicated by letters a, b, and not significant (ns).*

2.3.2.4. Necrosis (karyorrhexis)

Necrotic mesenterial filaments (mainly at the coelenteric cavities) (Figure 11E–F) were significantly more frequent in DA (87%) compared to DU (13%) and HH (0%), with no significant difference between DU and HH (Table 4). Notably, the prominent lytic necrosis of gastrodermis described in Landsberg et al. (2020) was not confirmed, and no remarkable findings were noted in the epidermis.

Health Status	Carysfort	Grecian/KLDR	Looe	Total
HH	0% (0/3)	0% (0/3)	0% (0/3)	0% (0/9) [a]
DU	40% (2/5)	0% (0/5)	0% (0/5)	13% (2/15)[a]
DA	100% (5/5)	60% (3/5)	100% (5/5)	87% (13/15)[b]
Total	54% (7/13) [ns]	23% (3/13) [ns]	38% (5/13)[ns]	38% (15/39)

Table 4. *Necrosis in the mesenterial filaments of* Orbicella faveolata*. Health conditions: HH, healthy; DU, disease unaffected; DA, disease affected. Fisher's Exact test adjusted p-value ($p < 0.05$) indicated by letters a, b, and not significant (ns).*

2.3.2.5. Mucus cell hypertrophy

Mucus cells in the mesenterial filaments (mainly at the coelenteric cavities) appeared to be enlarged and contained abundant mucus that stained prominently blue with thionin (Figure 12). This feature was confirmed in all health conditions; 11% (HH), 33% (DU), and 47% (DA), with no significant differences among them. Especially, granules containing mucin in the cnidoglandular band adjacent to the mesenterial filaments with hypertrophied mucus cell were observed to be dissociated.

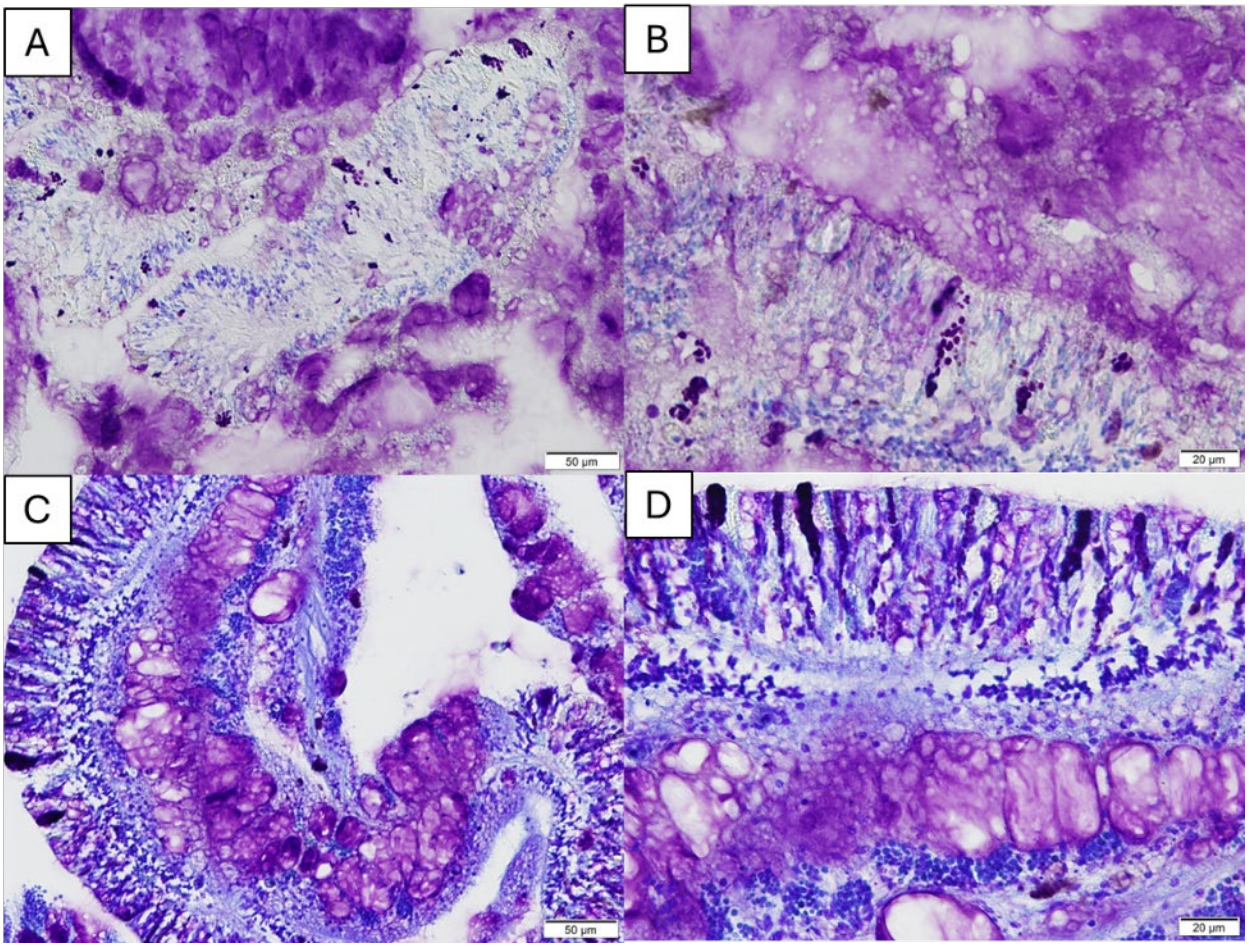

Figure 12. *Histological sections of* Orbicella faveolata *(thionin). (A) Mucus cell hypertrophy of mesenterial filament (mainly at the coelenteric cavities) in a disease affected colony from Grecian. Note that mucus stained lightly purple to slightly brownish color, and the granules containing mucin in the cnidoglandular band adjacent to the mesenterial filaments with hypertrophied mucus cell were observed to be dissociated. (B) High magnification image of (A). (C) Normal amount of mucus production of mesenterial filament (mainly at the coelenteric cavities) in a healthy colony from Grecian. Note that mucus stained dark purple, condensed appearance, and the granules containing mucin in the cnidoglandular band adjacent to the mesenterial filaments were observed to be tightly condensed. (D) High magnification image of (C).*

2.3.2.6. Periodic acid-Schiff (PAS)-positive reaction of endosymbionts

Starch granules in the cytoplasm of endosymbionts located in the surface body wall (SBW) of the gastrodermis stained strongly positive (red) with PAS-MY (Figure 13) in all specimens, except one from HH at the Carysfort South site (Table 5).

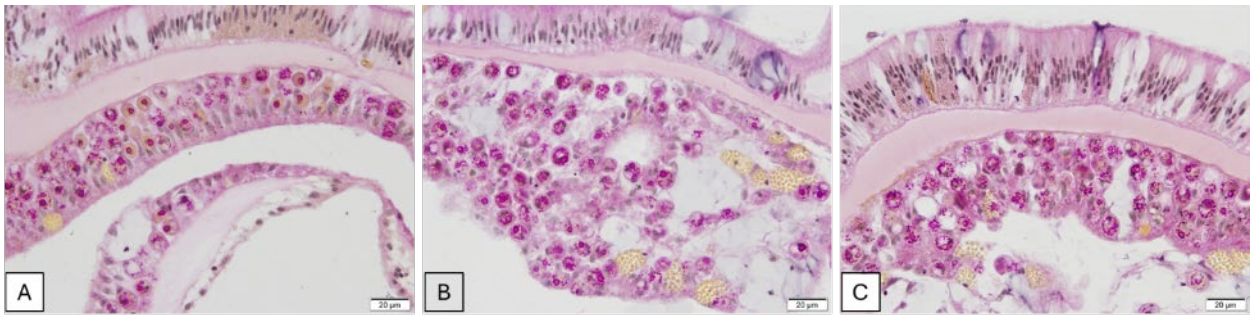

Figure 13. *Histological sections of surface body wall of the gastrodermis in* Orbicella faveolata*, showing endosymbiont starch granules with periodic acid-Schiff's reagent (PAS) stain reaction (PAS-MY). (A) Healthy core colony sample. (B) Disease unaffected core colony sample. (C) Disease affected core colony sample. All samples were obtained from Carysfort South.*

Health Status	Carysfort	Grecian/KLDR	Looe	Total
HH	67% (2/3)	100% (3/3)	100% (3/3)	89% (8/9)^{ns}
DU	100% (5/5)	100% (5/5)	100% (5/5)	100% (15/15) ^{ns}
DA	100% (5/5)	100% (5/5)	100% (5/5)	100% (15/15) ^{ns}
Total	92% (12/13) ^{ns}	100% (13/13) ^{ns}	100% (13/13)^{ns}	97% (38/39)

Table 5. *PAS (Period acid Schiff)-positive reaction of endosymbionts at surface gastrodermis. Health conditions: HH, healthy; DU, disease unaffected; DA, disease affected. Fisher's Exact test adjusted p-value ($p < 0.05$) indicated not significant (ns).*

2.3.2.7. Necrosis of endosymbiont (ghost)

Multifocal necrosis, exemplified as the retention of only the outer frame of the organismal body with loss of internal structures including the nucleus (referred to as ghosting) was found in the surface body wall of the gastrodermis (Figure 14). Endosymbionts exhibited somewhat swollen, light brownish-green tinted cytoplasm under H&E, absence of nuclei, and an enlarged symbiosome space that was expanded and coalesced. Necrosis of endosymbionts was significantly more frequent in DA (93%) and DU (60%) compared to HH (11%), but there was no statistical difference between DA and DU (Table 6).

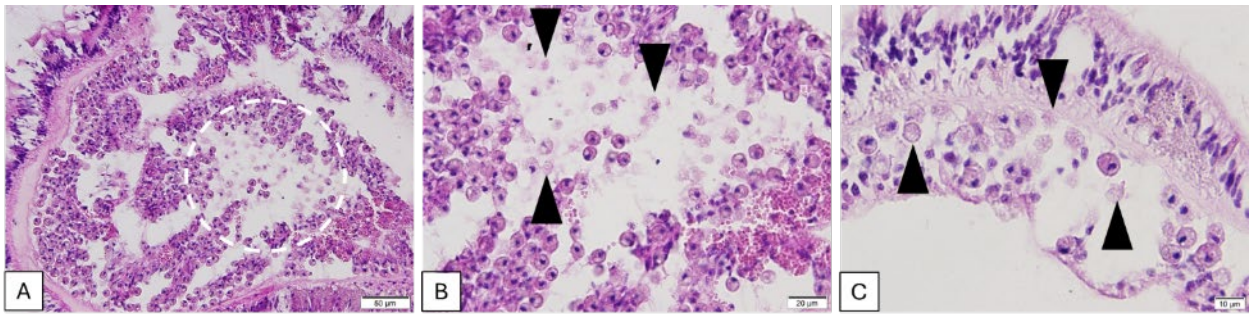

Figure 14. *Histological sections of* Orbicella faveolata *(H&E). (A) Focal necrosis of endosymbionts (dotted circle) in the surface body wall gastrodermis of a disease affected sample from Grecian. (B) High magnification of circle in (A) showing necrotic endosymbionts (arrowheads). (C) Another high magnification view of the gastrodermis showing necrotic endosymbionts (arrowheads) in a disease affected sample.*

Health Status	Carysfort	Grecian/KLDR	Looe	Total
HH	0% (0/3)	33% (1/3)	0% (0/3)	11% (1/9)[a]
DU	40% (2/5)	60% (3/5)	80% (4/5)	60% (9/15)[b]
DA	100% (5/5)	80% (4/5)	100% (5/5)	93% (14/15)[b]
Total	54% (7/13) [ns]	62% (8/13) [ns]	69% (9/13)[ns]	62% (24/39)

Table 6. *Proportion of samples exhibiting necrosis (ghost) of endosymbionts at surface gastrodermis. Health conditions: HH, healthy; DU, disease unaffected; DA, disease affected. Fisher's Exact test adjusted p-value ($p < 0.05$) indicated by letters a, b, and not significant (ns).*

2.3.2.8. Organisms detected

Coccidia were sporadically detected in the filaments regardless of health condition from Carysfort South (N = 3) and Looe Key (N = 4). Endolithic algae-hyphae were also sporadically and lightly detected. Possible rickettsia-like organisms (Figure 15), that stained magenta with Giemsa and had a coccoid-like appearance (described in Landsberg et al. 2020) were observed frequently in the surface body wall gastrodermis, but occasionally in the mesenterial filaments both protruded one those settled in a coelenteric cavity (Table 7).

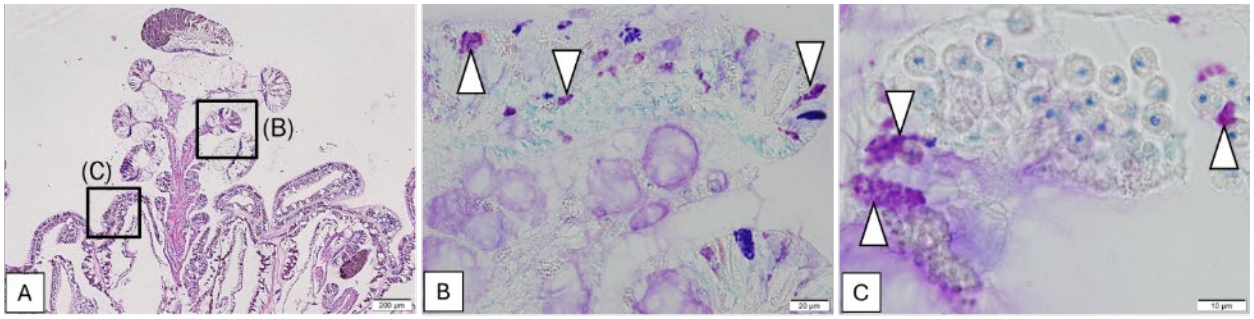

Figure 15. *Histological sections of* Orbicella faveolata *(H&E and Giemsa). (A) Mesenterial filaments protruded from surface epidermal tissue in a disease affected colony from Carysfort. DU. (B) Protruded mesenterial filaments and cnidoglandular, a*

magnified area of (B) in pane (A) showing coccoid-like Rickettsia-like organisms stained magenta (arrowheads). (C) Gastrodermis, magnified area of (C) in pane (A) showing coccoid-like Rickettsia-like organisms stained magenta (arrowheads).

Health Status	Carysfort	Grecian/KLDR	Looe	Total
HH	66% (2/3)	100% (3/3)	66% (2/3)	78% (7/9)[ns]
DU	100% (5/5)	80% (4/5)	100% (5/5)	93% (14/15) [ns]
DA	100% (5/5)	100% (5/5)	100% (5/5)	100% (15/15) [ns]
Total	92% (12/13) [ns]	92% (12/13) [ns]	92% (12/13)[ns]	92% (36/39)

Table 7. *Proportion of samples exhibiting coccoid-like organisms. Health conditions: HH, healthy; DU, disease unaffected; DA, disease affected. Fisher's Exact test adjusted p-value ($p < 0.05$) indicated by not significant (ns).*

2.3.3. Collaborative Meetings

We conducted semi-monthly meetings (August, October, December, February, April) and an in-person workshop to collaboratively advance the science of OATLD. Meetings consisted of each team sharing results to date and synthesizing observations. Results from NSU and FWC are reported above. Results from TEM and microbiome analyses are reported through the Ushijima and Meyer final DEP reports. Though not funded under this project, results from different groups have been presented at conferences, and manuscript preparation is underway.

2.4. Discussion & Management Recommendations

Through extensive collaborative assessments of OATLD, there appear to be fundamental differences between this disease and SCTLD. Disease lesions have a different appearance, halt on their own with some frequency, and have minimal response to amoxicillin. Prevalence on *O. faveolata* colonies demonstrates seasonal peaks in late summer, has been present in the Florida Keys since at least 2019, and, concerningly, seems to target the largest coral colonies. Histologically, OATLD does not show the characteristic trademarks of SCTLD such as lytic necrosis. TEM work done by the Ushijima lab at UNCW (and reported upon in their final report) also identifies notable differences between OATLD and SCTLD samples, including high numbers of starches and lipids within the symbionts of OATLD-affected corals, high numbers of accumulation bodies within those symbionts, and low numbers of broken-down symbionts. Microbiome studies conducted by the Meyer lab at UF (and reported upon in their final report) identified 10 bacterial ASVs that are enriched in both SCTLD and OATLD samples, and 5 that are more unique to OATLD only. Based on these conclusions, we suggest that OATLD is a distinct disease from SCTLD.

Though we concentrated primarily on comparisons to SCTLD, the collaborative group also began exploring comparisons of OATLD to various white plague syndromes. Similarities of OATLD to white plague include more similar lesion descriptions and

patterns of seasonality. Additionally, of the three microbial taxa enriched in OATLD which were not present in SCTLD, three of them have also been identified with white plague (see Meyer lab final report). Differences between OATLD and white plague, however, include the specificity of OATLD to *Orbicella faveolata* colonies, as well as lesions moving in various directions across the colonies as opposed to just from the bottom up. Comparisons of OATLD to white plague are complicated by the lack of histological and TEM work on white plague, which make those comparisons impossible. They are also complicated by the various forms of white plague that have been described which vary in their species affected as well as their progression rates. The histological assessment of presumed SCTLD lesions in the US Virgin Islands also complicates this story, as they do not conform to the established case definition of SCLTD (Work et al. 2025), but do have more similarity to some of the OATLD characteristics.

These lines of inquiry have produced a lengthy list of questions and next steps. However, the consortium agreed that the most pressing questions to answer are: 1) is OATLD transmissible (via physical contact and/or waterborne transmission), 2) are other species susceptible to OATLD in a transmission experiment, and 3) are there treatment options that can prevent mortality of these large corals to OATLD lesions. To that end, we recommend prioritizing funding and permitting to address these questions and potentially provide management tools to address this threat.

3. APPENDICES

3.1. Appendix I: Bleaching index data

Bleaching index scores for each coral during each monitoring period. Gray boxes indicate the coral was not found. Results are presented visually in Figures 4 and 5.

			Bleaching Index Score											
Tag #	Species	Treatment	7/8/2024	7/16/2024	8/17/2024	8/29/2024	9/13/2024	9/23/2024	10/1/2024	10/7/2024	10/14/2024	11/12/2024	12/19/2024	3/20/2025
967	PCLI	control	2.98	3.98	2.95	3.95	3.30	3.49	4.00	4.00	4.00	5.00	4.50	4.50
1110	PCLI	control	3.00	3.00	3.50	3.00	3.00	3.49	3.50		4.00	4.03	4.10	3.50
3449	PCLI	control	3.00	4.00	2.50	3.40	2.50	3.00	2.75	4.00	4.00	4.50	4.00	5.00
7709	PCLI	control	3.50	2.95	2.65	4.00	2.15	3.10	2.70	3.50	4.00	4.75	4.00	5.00
7921	PCLI	control	4.00	4.50	2.95	4.00	3.80	4.00	4.00	4.00	4.25	5.00	4.50	4.50
N-105	PCLI	control	4.00	4.00	3.50	4.00	3.00	3.50	3.75	4.00	4.00	4.98	4.00	4.00
N-106	PCLI	control	4.00	4.00	3.50	3.50	3.15	4.00	4.00	4.00	3.85	5.00	4.50	4.00
N-140	PCLI	control	3.00	3.50	3.50	3.00	3.00	3.40	3.50	4.00	4.25	4.75	4.00	4.50
N-143	PCLI	control	3.90	3.80	4.00	4.00	3.40	3.50	4.00	4.00	4.50	4.50	4.00	4.00
N-147	PCLI	control	4.00	4.50	4.00	4.00	4.00	4.00	4.00	4.00	5.00	5.00	4.50	5.00
N-149	PCLI	control	4.50	4.50	4.50	4.00	3.98	4.00	4.00	4.00	4.75	5.00	5.00	5.00
957	PCLI	shaded	4.00	4.00	4.00	4.00	4.00	4.00	4.50	5.00	4.25	5.00	4.50	4.50
963	PCLI	shaded	3.00	4.50	3.43	3.70	3.40	3.98	4.50	4.00	4.50	5.00	4.50	4.50
3444	PCLI	shaded	4.00	4.50	4.00	4.00	4.50	4.93	4.50	4.50	4.50	5.00	5.00	5.00
3448	PCLI	shaded	4.00	4.00	4.00	4.00	4.00	4.30	4.00	4.00	4.00	4.75	4.50	4.75
N-103	PCLI	shaded	4.00	4.00	3.00	4.00	3.50	4.00	4.25	4.00	4.00	5.00	4.50	5.00
N-104	PCLI	shaded	4.00	4.00	4.00	4.00	4.00	4.00	4.00	4.00	4.50	5.00	5.00	4.00
N-138	PCLI	shaded	3.00	4.00	3.00	4.00	3.50	4.30	4.00	4.00	4.00	5.00	5.00	4.50
N-142	PCLI	shaded	3.98	4.00	3.00	4.00	3.70	4.00	4.00	4.50	4.25	4.85	4.90	4.00
N-145	PCLI	shaded	4.00	4.00	3.00	4.00	4.00	4.00	3.30	4.50	3.93	4.90	4.50	5.00
N-83	PCLI	shaded	4.00	4.00	4.00	4.50	4.00	4.00	4.50	4.00	4.50	5.00	4.50	4.00
9292	CNAT	control	3.20	3.60	2.90	4.28	3.40	3.30	3.38	4.25	4.30	4.98	4.95	4.50
888	CNAT	control	3.00	4.50	4.00	4.00	3.50	3.00	4.00	4.00	4.50	5.00	4.50	4.00
934	CNAT	control	5.00	4.50	4.46	4.50	5.00	4.50	5.00	4.50	5.00	5.00	5.00	4.50
1242	CNAT	control	4.00	5.00	4.00	4.50	3.00	3.50	3.80	4.00	4.00	4.93	4.63	4.50
3438	CNAT	control	5.00	5.00	5.00	4.50	3.50	4.00	4.00	4.00	4.50	4.75	5.00	4.50
4377	CNAT	control	3.10	3.30	3.40	3.75	3.90	4.00	4.50	4.50	5.00	5.00	5.00	4.50
4501	CNAT	control	3.40	4.50	4.50	5.00	4.05	3.85	3.50	4.00	4.00	5.00	4.50	5.00
N-9	CNAT	control	3.50	4.50	4.00	4.50	4.00	4.50	4.50	5.00	5.00	5.00	5.00	4.50
N-47	CNAT	control	4.00	4.50	4.50	4.50	4.70	4.00	4.50	4.50	4.50	5.00	5.00	4.50
N-61	CNAT	control	5.00	4.90	4.35	4.43	4.10	4.00	4.50	5.00	5.50	5.00	4.35	4.50
N-100	CNAT	control	3.25	3.70	3.50	3.90	3.99	4.00	4.25	4.50	4.00	5.00	5.00	4.50

890	CNAT	shaded	4.00	5.00	4.00	4.50	5.46	4.50	4.00	4.00	5.00	5.00	5.00	5.00
894	CNAT	shaded	5.00	5.00	5.00	5.00	4.50	5.00	4.50	5.00	5.50	5.00	5.00	4.50
1313	CNAT	shaded	4.00	5.00	4.50	5.00	4.00	5.00	4.25	5.00	4.00	4.75	5.00	5.00
3443	CNAT	shaded	5.00	5.00	4.63	4.50	4.50	4.50	5.00	4.50	4.00	5.00	4.80	4.50
4799	CNAT	shaded	3.00	3.45	4.00	4.00	4.50	5.00	4.50	5.00	5.00	5.00	5.00	5.00
8776	CNAT	shaded	3.30	3.80	4.00	4.00	5.50	4.50	5.00	5.00				
9080	CNAT	shaded	4.00	4.00	4.50	4.00	4.50	5.00	5.00	5.00	5.75	5.00	5.00	5.00
N-37	CNAT	shaded	4.00	4.50	4.20	4.50	4.00	4.00	4.20	4.50	4.50	5.00	4.80	4.00
N-63	CNAT	shaded	5.00	5.00	5.00	5.00	4.50	4.00	4.00	5.00	4.00	5.00	5.00	4.50
N-64	CNAT	shaded	4.00	5.00	4.00	4.50	5.00	5.00	5.25	5.00	5.00	5.00	4.95	4.50

3.2 Appendix II: OATLD data (from Figure 8)

8A: Status of lesions ~2 months after initial assessments

	Halted	% Active	Consumed all Tissue
Looe	47% (21/45)	27% (12/45)	27% (12/45)
Grecian/KLDR	55% (21/38)	32% (12/38)	13% (5/38)
Carysfort	31% (12/39)	56% (22/39)	13% (5/39)

8B: Proportion of OATLD lesions halted during each monitoring period

Site	Dates	# Measured Lesions	# Halted Lesions	% Halted Lesions
Looe	1/31/2024	14	13	92.9
Looe	2/16-2/25/24	12	6	50.0
Looe	4/6/2024	2	2	100.0
Looe	5/8-5/13/24	2	0	0.0
Looe	7/8/2024	1	0	0.0
Looe	9/9/2024	4	4	100.0
Looe	1/19/2025	2	0	0.0
Grecian/KLDR	1/11-1/30/24	9	4	44.4
Grecian/KLDR	4/5/2024	12	10	83.3
Grecian/KLDR	5/21/2024	2	0	0.0
Grecian/KLDR	7/18/2024	8	7	87.5
Grecian/KLDR	9/16/2024	2	0	0.0
Grecian/KLDR	11/24/2024	4	3	75.0
Carysfort	1/28/2024	14	0	0.0
Carysfort	4/5/2024	9	3	33.3
Carysfort	5/21/2024	4	3	75.0
Carysfort	7/18/2024	4	2	50.0
Carysfort	9/16/2024	3	1	33.3
Carysfort	11/24/2024	4	3	75.0
Carysfort	1/28/2025	4	2	50.0

8C: Lesion progression rates of OATLD lesions by site.

	Avg	St Dev	N
Looe	0.44	0.27	12
Grecian/KLDR	0.47	0.24	12
Carysfort	0.41	0.17	21

8D: Amoxicillin efficacy on OATLD lesions by site and time frame

		# Assessed treatments	# Effective Treatments	% Efficacy
Looe	2019-2020	9	3	33%
	2022-2023	5	1	20%
Sombrero	2019-2020	12	7	58%
	2022-2023	2	0	0%
Molasses	2019-2020	6	2	33%
	2022-2023	0	N/A	N/A
Carysfort	2019-2020	10	4	40%
	2022-2023	11	0	0%
Cheeca	2019-2020	6	2	33%
	2022-2023	5	3	60%

8E: Disease type on the first 40 first treated colonies at each site (34 at Molasses).

	OATLD	SCTLD + OATLD	SCTLD
Looe	5	0	35
Sombrero	8	2	30
Molasses	14	1	19
Carysfort	12	3	25
Marker 48	2	0	38
Cheeca Rocks	6	1	33

8F: Maximum diameter (cm) of *Orbicella faveolata* colonies affected by OATLD versus that of corals affected by SCTLD.

	OATLD			SCTLD		
	Avg	St Dev	N	Avg	St Dev	N
Sand Key	171	96	40	115	86	90
Looe Key	197	83	168	169	76	548
Sombrero	157	93	22	121	73	56

3.3 Appendix III: OATLD prevalence data

Prevalence of OATLD on *Orbicella faveolata* colonies with known susceptibility to white disease. Tables are separated by site (Sand, Looe, Sombrero). Results are presented visually in Figure 9.

Sand	2019	2020	2021	2022	2023
Jan		0.000			
Feb		0.000		0.019	
Mar			0.000		0.020
Apr		0.000		0.009	
May			0.019		0.000
Jun		0.018			
Jul			0.075		
Aug		0.000		0.037	
Sep			0.112		
Oct	0.000	0.036		0.019	
Nov	0.000		0.084		
Dec		0.065		0.019	

Looe	2019	2020	2021	2022	2023
Jan				0.021	
Feb		0.003	0.006		0.012
Mar		0.001		0.011	
Apr			0.009		0.002
May		0.006		0.007	
Jun			0.003		0.002
Jul		0.018			
Aug			0.017	0.012	
Sep		0.011			
Oct			0.036	0.030	
Nov		0.018			
Dec	0.001			0.042	

Sombrero	2019	2020	2021	2022	2023
Jan		0.026	0.121		
Feb				0.042	
Mar	0.013		0.042		0.000
Apr		0.039			
May	0.026		0.028	0.058	0.000
Jun		0.122			
Jul	0.014		0.055		
Aug		0.133		0.071	

Sep	0.013				
Oct		0.152	0.091	0.074	
Nov	0.026				
Dec			0.000	0.015	

4. REFERENCES

Aeby, G., B. Ushijima, E. Bartels, C. Walter, J. Kuehl, S. Jones, and V. J. Paul. 2021. Changing stony coral tissue loss disease dynamics through time in *Montastraea cavernosa*. Frontiers in Marine Science **8**:699075.

Aronson, R. B., and W. F. Precht. 2001. White-band disease and the changing face of Caribbean coral reefs. The ecology and etiology of newly emerging marine diseases:25-38.

Burke, S., P. Pottier, M. Lagisz, E. L. Macartney, T. Ainsworth, S. M. Drobniak, and S. Nakagawa. 2023. The impact of rising temperatures on the prevalence of coral diseases and its predictability: A global meta-analysis. Ecology letters **26**:1466-1481.

Butcherine, P., A. Tagliafico, S. L. Ellis, B. P. Kelaher, C. Hendrickson, and D. Harrison. 2023. Intermittent shading can moderate coral bleaching on shallow reefs. Frontiers in Marine Science **10**:1162896.

Coelho, V., D. Fenner, C. Caruso, B. Bayles, Y. Huang, and C. Birkeland. 2017. Shading as a mitigation tool for coral bleaching in three common Indo-Pacific species. Journal of Experimental Marine Biology and Ecology **497**:152-163.

Gignoux-Wolfsohn, S. A., W. F. Precht, E. C. Peters, B. E. Gintert, and L. S. Kaufman. 2020. Ecology, histopathology, and microbial ecology of a white-band disease outbreak in the threatened staghorn coral *Acropora cervicornis*. Diseases of aquatic organisms **137**:217-237.

Gladfelter, W. B. 1982. White-band disease in *Acropora palmata*: implications for the structure and growth of shallow reefs. Bulletin of marine Science **32**:639-643.

Hawthorn, A. C., M. Dennis, Y. Kiryu, J. Landsberg, E. Peters, and T. M. Work. 2024. Stony coral tissue loss disease (SCTLD) case definition for wildlife.

Jeans, J., D. A. Campbell, and M. O. Hoogenboom. 2013. Increased reliance upon photosystem II repair following acclimation to high-light by coral-dinoflagellate symbioses. Photosynthesis research **118**:219-229.

Kayanne, H. 2017. Validation of degree heating weeks as a coral bleaching index in the northwestern Pacific. Coral Reefs **36**:63-70.

Landsberg, J. H., Y. Kiryu, E. C. Peters, P. W. Wilson, N. Perry, Y. Waters, K. E. Maxwell, L. K. Huebner, and T. M. Work. 2020. Stony coral tissue loss disease in Florida is associated with disruption of host–zooxanthellae physiology. Frontiers in Marine Science **7**:576013.

Levitan, D. R., W. Boudreau, J. Jara, and N. Knowlton. 2014. Long-term reduced spawning in Orbicella coral species due to temperature stress. Marine Ecology Progress Series **515**:1-10.

Manzello, D. 2015. Rapid recent warming of coral reefs in the Florida Keys. Sci Rep 5: 16762.

Maynard, J., R. Van Hooidonk, C. M. Eakin, M. Puotinen, M. Garren, G. Williams, S. F. Heron, J. Lamb, E. Weil, and B. Willis. 2015. Projections of climate conditions that increase coral disease susceptibility and pathogen abundance and virulence. Nature Climate Change **5**:688-694.

Mellin, C., S. Brown, N. Cantin, E. Klein-Salas, D. Mouillot, S. F. Heron, and D. A. Fordham. 2024. Cumulative risk of future bleaching for the world's coral reefs. Science Advances **10**:eadn9660.

Muller, E. M., E. Bartels, and I. B. Baums. 2018. Bleaching causes loss of disease resistance within the threatened coral species Acropora cervicornis. Elife **7**:e35066.

Neely, K. L., C. L. Lewis, K. S. Lunz, and L. Kabay. 2021a. Rapid population decline of the pillar coral *Dendrogyra cylindrus* along the Florida Reef Tract. Frontiers in Marine Science **8**:656515.

Neely, K. L., R. J. Nowicki, M. A. Dobler, A. A. Chaparro, S. M. Miller, and K. A. Toth. 2024. Too hot to handle? The impact of the 2023 marine heatwave on Florida Keys coral. Frontiers in Marine Science **11**:1489273.

Neely, K. L., C. P. Shea, K. A. Macaulay, E. K. Hower, and M. A. Dobler. 2021b. Short- and long-term effectiveness of coral disease treatments. Frontiers in Marine Science **8**:675349.

Papke, E., G. E. Kennedy, E. Elliott, A. Taylor, B. B. Tolar, and B. Ushijima. 2024. Transmission Electron Microscopy of Coral Tissue. Current Protocols **4**:e70033.

Porter, J. W., P. Dustan, W. C. Jaap, K. L. Patterson, V. Kosmynin, O. W. Meier, M. E. Patterson, and M. Parsons. 2001. Patterns of spread of coral disease in the Florida Keys. The ecology and etiology of newly emerging marine diseases:1-24.

Quintero-Hunter, I., H. Grier, and M. Muscato. 1991. Enhancement of histological detail using metanil yellow as counterstain in periodic acid Schiff's hematoxylin staining of glycol methacrylate tissue sections. Biotechnic & Histochemistry **66**:169-172.

Richardson, L. L. 1998. Coral diseases: what is really known? Trends in ecology & evolution **13**:438-443.

Rogers, C. S. 2010. Words matter: recommendations for clarifying coral disease nomenclature and terminology. Diseases of aquatic organisms **91**:167-175.

Tagliafico, A., P. Baker, B. Kelaher, S. Ellis, and D. Harrison. 2022. The effects of shade and light on corals in the context of coral bleaching and shading technologies. Frontiers in Marine Science **9**:919382.

Toth, K. A., S. F. Buckley, H. Noren, K. L. Neely, and B. K. Walker. 2024. Broadscale coral disease interventions elicit efficiencies in endemic disease response. Frontiers in Marine Science **10**:1302697.

Ushijima, B., J. L. Meyer, S. Thompson, K. Pitts, M. F. Marusich, J. Tittl, E. Weatherup, J. Reu, R. Wetzell, and G. S. Aeby. 2020. Disease diagnostics and potential coinfections by *Vibrio coralliilyticus* during an ongoing coral disease outbreak in Florida. Frontiers in Microbiology **11**:569354.

Weil, E. 2004. Coral reef diseases in the wider Caribbean. Pages 35-68 Coral health and disease. Springer.

Work, T. M., J. Miller, T. Kelley, A. Hawthorn, T. Weatherby, and C. S. Rogers. 2025. Pathology of lesions in corals from the US Virgin Islands after emergence of stony coral tissue loss disease. Coral Reefs **44**:179-192.